

This is a repository copy of *Tuning the selectivity of natural oils and fatty acids/esters deoxygenation to biofuels and fatty alcohols : A review.*

White Rose Research Online URL for this paper:  
<https://eprints.whiterose.ac.uk/186490/>

Version: Published Version

---

**Article:**

Zhou, Yingdong, Remón, Javier [orcid.org/0000-0003-3315-5933](https://orcid.org/0000-0003-3315-5933), Jiang, Zhicheng et al. (2 more authors) (2022) Tuning the selectivity of natural oils and fatty acids/esters deoxygenation to biofuels and fatty alcohols : A review. Green Energy and Environment. ISSN 2468-0257

<https://doi.org/10.1016/j.gee.2022.03.001>

---

**Reuse**

This article is distributed under the terms of the Creative Commons Attribution-NonCommercial-NoDerivs (CC BY-NC-ND) licence. This licence only allows you to download this work and share it with others as long as you credit the authors, but you can't change the article in any way or use it commercially. More information and the full terms of the licence here: <https://creativecommons.org/licenses/>

**Takedown**

If you consider content in White Rose Research Online to be in breach of UK law, please notify us by emailing [eprints@whiterose.ac.uk](mailto:eprints@whiterose.ac.uk) including the URL of the record and the reason for the withdrawal request.



## Review article

# Tuning the selectivity of natural oils and fatty acids/esters deoxygenation to biofuels and fatty alcohols: A review

Yingdong Zhou<sup>a</sup>, Javier Remón<sup>b,e,\*</sup>, Zhicheng Jiang<sup>c,d</sup>, Avtar S. Matharu<sup>e</sup>, Changwei Hu<sup>a,\*</sup>

<sup>a</sup> Key Laboratory of Green Chemistry and Technology, Ministry of Education, College of Chemistry, Sichuan University, Chengdu, Sichuan 610064, China

<sup>b</sup> Instituto de Carboquímica, CSIC, Zaragoza, 50018, Spain

<sup>c</sup> Department of Biomass Science and Engineering, Sichuan University, Chengdu, 610064, China

<sup>d</sup> National Engineering Research Center of Clean Technology in Leather Industry, Sichuan University, Chengdu, 610064, China

<sup>e</sup> Green Chemistry Centre of Excellence, Department of Chemistry, University of York, Heslington, York, YO10 5DD, UK

Received 3 January 2022; revised 20 February 2022; accepted 3 March 2022

Available online ■ ■ ■

## Abstract

The chemical transformation of natural oils provides alternatives to limited fossil fuels and produces compounds with added value for the chemical industries. The selective deoxygenation of natural oils to diesel-ranged hydrocarbons, bio-jet fuels, or fatty alcohols with controllable selectivity is especially attractive in natural oil feedstock biorefineries. This review presents recent progress in catalytic deoxygenation of natural oils or related model compounds (e.g., fatty acids) to renewable liquid fuels (green diesel and bio-jet fuels) and valuable fatty alcohols (unsaturated and saturated fatty alcohols). Besides, it discusses and compares the existing and potential strategies to control the product selectivity over heterogeneous catalysts. Most research conducted and reviewed has only addressed the production of one category; therefore, a new integrative vision exploring how to direct the process toward fuel and/or chemicals is urgently needed. Thus, work conducted to date addressing the development of new catalysts and studying the influence of the reaction parameters (e.g., temperature, time and hydrogen pressure) is summarized and critically discussed from a green and sustainable perspective using efficiency indicators (e.g., yields, selectivity, turnover frequencies and catalysts lifetime). Special attention has been given to the chemical transformations occurring to identify key descriptors to tune the selectivity toward target products by manipulating the reaction conditions and the structures of the catalysts. Finally, the challenges and future research goals to develop novel and holistic natural oil biorefineries are proposed. As a result, this critical review provides the readership with appropriate information to selectively control the transformation of natural oils into either biofuels and/or value-added chemicals. This new flexible vision can help pave the way to suit the present and future market needs.

© 2022 Institute of Process Engineering, Chinese Academy of Sciences. Publishing services by Elsevier B.V. on behalf of KeAi Communications Co., Ltd. This is an open access article under the CC BY-NC-ND license (<http://creativecommons.org/licenses/by-nc-nd/4.0/>).

**Keywords:** Natural oil; Deoxygenation; Controllable selectivity; Biofuels; Fatty alcohols

## 1. Introduction

As the global population, industrialization and urbanization continue to increase, our need for energy and resources becomes ever-so-important [1,2]. By 2050, world energy

consumption is expected to rise approximately 50% [3]. However, the continued use of fossil fuels for our chemicals, materials and energy needs is unsustainable because of their limited supply and adverse environmental impact resulting in global warming and climate change [4,5]. Thus, we need to seek renewable alternatives (biomass) to fossil fuels for our energy and raw materials, along with environmentally benign processes, to mitigate climate change [6,7].

Biomass has gained sufficient attention globally due to its abundance, renewability and ability to sequester greenhouse

\* Corresponding authors. Instituto de Carboquímica, CSIC, Zaragoza, 50018, Spain..

E-mail addresses: [jremon@icb.csic.es](mailto:jremon@icb.csic.es) (J. Remón), [changwei@scu.edu.cn](mailto:changwei@scu.edu.cn) (C. Hu).

<https://doi.org/10.1016/j.gee.2022.03.001>

2468-0257/© 2022 Institute of Process Engineering, Chinese Academy of Sciences. Publishing services by Elsevier B.V. on behalf of KeAi Communications Co., Ltd. This is an open access article under the CC BY-NC-ND license (<http://creativecommons.org/licenses/by-nc-nd/4.0/>).

Please cite this article as: Y. Zhou et al., Tuning the selectivity of natural oils and fatty acids/esters deoxygenation to biofuels and fatty alcohols: A review, Green Energy & Environment, <https://doi.org/10.1016/j.gee.2022.03.001>

gas (GHG) emissions [8,9]. Biomass can be converted (valorized) into chemicals, materials and (bio)energy using appropriate technologies within the context of a biorefinery [10–12]. Commonly, biomass feedstocks include conventional crops (first generation), lignocellulosic wastes (second generation) and algae (third-generation) [13–19]. Among these, natural oils and fats, such as plant oils, animal fats and algal lipids, as well as waste cooking oils (WCO), have the potential to be transformed into sulfur- and nitrogen-free liquid biofuels and oxygen-containing chemicals [20,21]. Typically, natural oils comprise triglycerides (glycerol and fatty acids) and free fatty acids containing 8–24 carbon atoms (Table 1) [22–26]. Due to the similarity in the chemical composition and molecular structure of certain natural oils to fossil-derived gasoline/diesel fuels, their transformation into biobased liquid fuels is a feasible and sustainable proposition.

Historically, considerable effort has been put into transforming natural oils into first-generation biodiesel as a sustainable alternative to petroleum diesel (pure and/or blended) [35,36]. Biodiesel, i.e., fatty acid alkyl esters, is usually produced from the transesterification of triglycerides with an appropriate alcohol, typically methanol or ethanol [37–39]. In addition, biodiesel is recognized as an attractive alternative because of its sustainability, biodegradability and clean-burning properties [40]. However, the primary defects of biodiesel are its high viscosity, poor cold flow properties, and low energy density, which limit its direct application in diesel engines [34]. However, another approach to transforming natural oils to bioenergy is via their catalytic, selective, deoxygenation into liquid hydrocarbon fuels, i.e., the so-called second-generation biodiesel or green diesel. Compared to first-generation biodiesel, green diesel has zero oxygen content, better stability, higher heating value, higher cetane number and better cold flow properties, which results

in improved performance in diesel engines [41]. In addition to green diesel, natural oils are also suitable for producing bio-jet fuels via hydrodeoxygenation, hydrocracking and/or hydroisomerization [42].

However, the conversion of biomass into biofuels alone may not be economically viable [43,44]. Finding potential value-added products during the deoxygenation of natural oils in addition to the production of liquid hydrocarbon fuels becomes important within the context of an economically viable, zero-waste biorefinery that maximizes chemical opportunity from its source feedstock into multiple outputs. For example, in the hydrogenation process of natural oils/fatty acids, fatty alcohols, i.e., partial hydrogenation intermediates, are highly valued in the chemical industries as they find applications in manufacturing solvents, plasticizers, detergents and cosmetics [45,46]. However, most of the recent works published to date have focused on the deoxygenation of natural oils for energy applications (biofuels production). Therefore, the selective and cost-efficient production of fatty alcohols needs to be further developed.

Several recent research and review articles have mentioned the importance of catalytic activity in natural oil or fatty acid deoxygenation [47–49]. In addition to catalytic activity, the selectivity to target products for natural oil conversion is equally and even more significant for developing future biorefineries. However, all recent reviews and research articles have only focused on producing one category of products from natural oil deoxygenation, i.e., hydrocarbon fuels or fatty alcohols [41,50–56]. To the best of our knowledge, the role of catalyst properties and reaction conditions for controlling the selectivity of natural oil deoxygenation toward one or another category has not yet been critically reviewed. Thus, this review focuses on the latest development, along with challenges and opportunities in designing appropriate heterogeneous catalysts

Table 1  
Exemplar biobased feedstocks and their fatty acid composition.

Fatty acid	Structure	Fatty acid composition (wt.%)							
		Coconut	Algae	Palm	Jatropha	Soybean	Sunflower	Rapeseed	WCO <sup>a</sup>
Octanoic	C8:0 <sup>b</sup>	7.1	0.0	0.0	0.0	0.0	0.0	0.0	0.0
Capric	C10:0	5.8	0.0	0.0	0.0	0.0	0.0	0.0	0.0
Lauric	C12:0	52.8	0.0	0.0	0.0	0.0	0.0	0.0	0.1
Myristic	C14:0	18.9	0.1	0.0	0.0	0.1	0.1	0.1	4.2
Palmitic	C16:0	8.3	4.4	43.5	20.2	11.2	5.9	5.5	16.9
Palmitoleic	C16:1	0.0	0.0	0.0	0.0	0.0	0.1	0.4	0.5
Steric	C18:0	6.1	4.4	4.6	7.2	3.8	3.8	2.0	8.9
Oleic	C18:1	0.0	32.2	38.9	39.8	24.8	29.9	60.0	33.5
Linoleic	C18:2	0.0	56.2	10.4	31.5	51.8	58.7	20.3	35.5
Linolenic	C18:3	0.0	0.0	0.0	0.0	5.2	0.2	8.8	0.0
Arachidic	C20:0	0.0	0.0	0.0	0.0	0.5	0.3	3.0 <sup>c</sup>	0.2
Eicosenoic	C20:1	0.0	0.0	0.0	0.0	0.0	0.1	0.0	0.1
Behenic	C22:0	0.0	0.4	0.0	0.0	0.5	0.7	0.0	0.0
Erucic	C22:1	0.0	1.0	0.0	0.0	0.0	0.0	0.0	0.0
Lignoceric	C24:0	0.0	0.4	0.0	0.0	0.2	0.2	0.0	0.0
Ref.		[27]	[28]	[29]	[30]	[31]	[32]	[33]	[34]

<sup>a</sup> Waste cooking oil.

<sup>b</sup> Fatty acid with 8 carbon atoms and zero C=C double bonds.

<sup>c</sup> 3 wt% of fatty acid with more than 20 carbon numbers.

for the selective deoxygenation of natural oils and fatty acids to produce either biofuels or value-added chemicals. In particular, special emphasis has been given to understanding how and to what extent the active sites, metal-support interactions, defects, as well as the reaction conditions influence the reaction pathway. This information has been gathered from both experimental techniques and theoretical calculations according to recent studies. As a result, this critical review collects essential information on the reaction pathways and mechanisms describing the deoxygenation of natural oils to provide the readership with relevant details to selectively control the transformation of these species into either biofuels (including diesel-ranged alkanes and bio-jet fuels) or value-added chemicals (fatty alcohols). This is very timely and helps to gain the full potential of these feedstocks and adapt their valorization to present and future market needs.

## 2. Deoxygenation pathways of natural oils

The deoxygenation process of natural oils includes liquid phase and gaseous phase reactions. In general, liquid phase reactions include elementary steps such as hydrogenolysis, hydrogenation, decarbonylation (DCO), decarboxylation (DCO<sub>2</sub>) and hydrodeoxygenation (HDO) [57,58]. The pathway to products in liquid phase reactions is slightly different depending on the reactant species within any given biobased feedstock. For example, triglycerides are the main components of vegetable oils (palm oil and olive oil), animal fats and algal oil [59–61]; free fatty acids mainly exist in the triglyceride hydrolysate, waste refining oils, or a small fraction in natural oils [62–64]; and fatty acid esters are commonly present in biodiesel [65]. The gaseous phase products from the deoxygenation reaction might include H<sub>2</sub>, CO<sub>2</sub>, CO, CH<sub>4</sub>, and H<sub>2</sub>O, produced via the dehydrogenation, DCO<sub>2</sub>, DCO, methanation or water-gas shift reactions [21,66,67]. This section focuses on the liquid phase reaction pathways only.

A schematic reaction pathway for the deoxygenation of natural oil-derived compounds is illustrated in Fig. 1. In recent studies, triglycerides, fatty acids and fatty esters have been commonly used as model compounds for natural oils due to their structural similarities. The deoxygenation of, for example, an unsaturated triglyceride can undergo different transformations, including hydrogenation,  $\gamma$ -H migration, hydrolysis and hydrogenolysis. The C=C double bonds can be reduced to form saturated triglycerides (also as one potential feedstock) in the presence of a hydrogen source, which can undergo a subsequent hydrogenolysis to produce three moles of saturated fatty acid and one mole of propane [68,69].

For these transformations, the hydrogen source can either be molecular hydrogen or a latent source, e.g., formic acid, methanol or isopropanol [70,71]. Besides, the saturated fatty acid can also be decarboxylated to C<sub>n-1</sub> alkane in the absence of H<sub>2</sub>, releasing carbon dioxide. In addition, the formed fatty acid can undergo further reduction (hydrogenation) to form an intermediate, partially reduced aldehyde but generally gives the fully reduced saturated fatty alcohol, an attractive commercial product. This fatty aldehyde intermediate is unstable under the reaction conditions and is quickly hydrogenated to the more stable fatty alcohol, which could be a potential product [72]. The oxygen atoms of the fatty aldehyde and fatty alcohol are subsequently removed via two parallel deoxygenation pathways (Fig. 1): (1) the DCO of the fatty aldehyde to a C<sub>n-1</sub> alkane and carbon monoxide; and (2) the HDO of the fatty alcohol intermediate to a C<sub>n</sub> alkane and H<sub>2</sub>O. These C<sub>n-1</sub> and C<sub>n</sub> alkanes are usually diesel-ranged paraffins with straight chains, where the carbon numbers depend on the original triglyceride used as a feedstock. The formed n-alkane products can further go through side reactions such as hydrocracking, isomerization, and aromatization, forming shorter-chain alkanes, branched alkanes, and arenes. These mixtures of hydrocarbons could be used as aviation fuel, also known as bio-jet fuel [47,49].

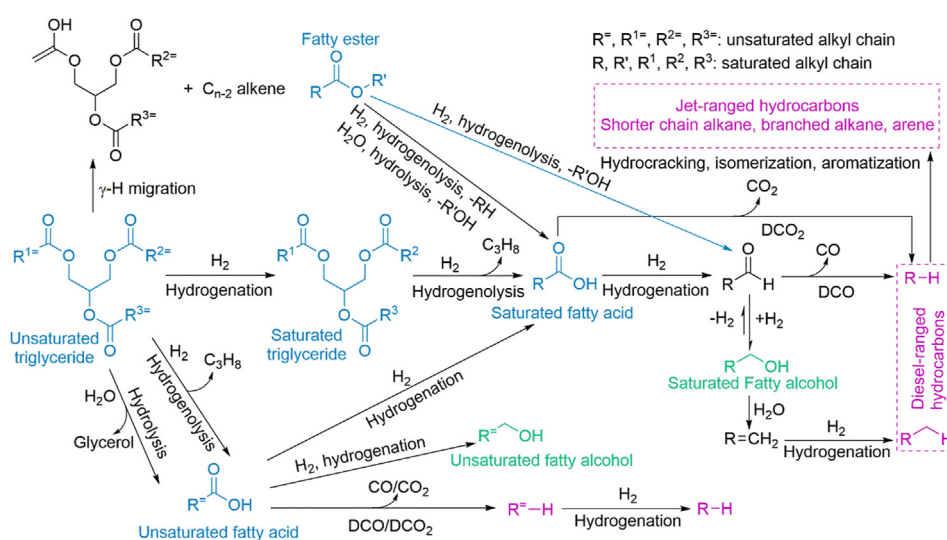


Fig. 1. Deoxygenation pathways of natural oil-derived compounds.

Concerning hydrolysis and hydrogenolysis, the C–O bond cleavage of an unsaturated triglyceride affords an unsaturated fatty acid, with glycerol (hydrolysis) or propane (hydrogenolysis) as a byproduct. The resultant unsaturated fatty acid can undergo further transformations, for example, hydrogenation, leading to a saturated fatty acid and/or one (un)saturated fatty alcohol. In parallel,  $C_{n-1}$  alkenes can also be formed via dehydrogenation, DCO and DCO<sub>2</sub>, releasing CO and CO<sub>2</sub>, respectively, which can then be hydrogenated to yield saturated alkanes [73]. Alternatively, triglycerides can be thermally decomposed via  $\gamma$ -H migration, resulting in the generation of  $C_{n-2}$  alkenes. This reaction usually occurs at relatively high temperatures between 250 and 380 °C [58].

Generally, saturated fatty acids are produced from unsaturated triglycerides. As discussed above, these can be deoxygenated via hydrogenation, followed by DCO<sub>2</sub>, DCO and HDO routes. For unsaturated fatty acids, these species can be hydrogenated to saturated fatty acids initially, and proceed via the abovementioned transformations. Another hydrogenation route for unsaturated fatty acids is selectively removing the oxygen atoms without losing the unsaturation, i.e., forming unsaturated fatty alcohols (e.g., oleyl alcohol) as a product. Unsaturated fatty alcohols are valuable chemicals with applications as lubricants and plasticizers [45,74]. Since the structure of fatty esters is similar to triglycerides (long carbon chain and ester bond), they can also be used as the model compounds in deoxygenation reactions to produce alkanes or fatty alcohols. The first step comprises the fatty acid formation via hydrolysis in the presence of water, generating an alcohol as a byproduct. The formed fatty acid undergoes the abovementioned deoxygenation pathways. Another possible route for a fatty ester is the initial hydrogenolysis to a fatty aldehyde or fatty acid, releasing an alcohol or alkane, followed by DCO or HDO to produce alkanes [20,21].

In catalytic transfer hydrogenation under a hydrogen-free atmosphere, the hydrogen donor (e.g., formic acid, methanol and isopropanol) undergoes a dehydrogenation or reforming reaction to produce H<sub>2</sub> or H atoms in situ in the presence of a suitable catalyst (Fig. 2). As the hydrogenation of natural oils requires H<sub>2</sub> or H atoms, the deoxygenation pathway in Fig. 1 is still valid for the transfer hydrogenation.

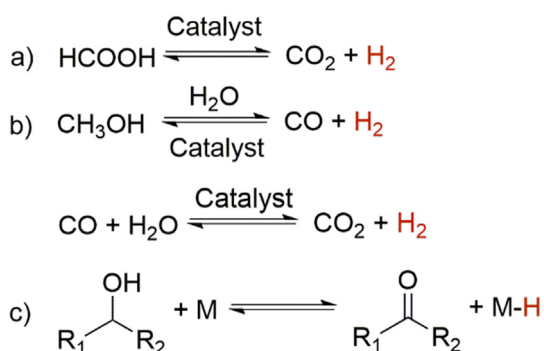


Fig. 2. Hydrogen formation pathways from (a) formic acid, (b) methanol and (c) isopropanol (where  $R_1 = R_2 = \text{CH}_3$ ), during the catalytic transfer hydrogenation [71,75,76].

### 3. Liquid hydrocarbon fuel production

Liquid hydrocarbon fuel is one of the most common products from the deoxygenation of natural oils. As discussed in the previous section, the main products are *n*-alkanes, cracking alkanes, branched alkanes, and aromatic hydrocarbons (Fig. 1). Due to the long carbon chains ( $C_8$ – $C_{24}$ ,  $C_{12}$ – $C_{18}$  in high fraction) in natural fatty acids, these *n*-alkanes are commonly in the diesel range, while cracking alkanes, branched alkanes, and aromatic hydrocarbons are considered jet-ranged biofuels [77,78]. Catalysts play a crucial role in the extension of chemical reactions taking place during the deoxygenation process. For example, metal- and non-metal-based (heterogeneous) catalysts have typically been used to remove the oxygen atoms in natural oil molecules. In recent years, various metal-based catalysts have been investigated for the deoxygenation of natural oils, including metal-non-metal nanocrystals (e.g., metal sulfides/phosphides/carbides) [79–81], noble metals (e.g., Pt, Pd, and Ru) [82–85], and non-noble metals (e.g., Ni, Co, Fe, and Mo) [86–89]. These have been supported over several materials, i.e., supports, with different physicochemical properties to disperse the metal particles. Depending on the active phases and supports, different metal-support interactions, influencing the catalytic activity and product selectivity, occur. This section critically reviews the catalytic activity of different types of active metals supported catalysts used to date for the production of liquid hydrocarbon fuels from natural oils.

#### 3.1. Diesel-ranged hydrocarbons

Diesel-ranged hydrocarbons are formed from the DCO<sub>2</sub>, DCO or HDO reactions of natural oils. Among these reactions, HDO consumes more hydrogen but exhibits a higher atom economy. On the contrary, DCO and DCO<sub>2</sub> are more hydrogen-economical but produce non-ecofriendly CO<sub>2</sub> and CO, thus hampering the carbon balance of the liquid phase. The catalyst plays a crucial role in these reactions. Different types of metal-based catalysts and supports promote different deoxygenation pathways (HDO, DCO and DCO<sub>2</sub>). Therefore, it is paramount to design catalysts with good physicochemical properties to maximize the selectivity toward desired products and avoid side reactions resulting in significant carbon loss. The catalysts used to date and their selectivity and peculiarities are described as follows.

##### 3.1.1. Metal sulfide/phosphide/carbide catalysts

Metal-non-metal nanocrystals (e.g., metal sulfides, metal phosphides and metal carbides) have been proven to be effective in several thermochemical processes, and even in electrochemical and photochemical reactions [90,91]. In this regard, metal sulfide catalysts have been widely applied in the petroleum industries for hydrodesulfurization, hydrodenitrogenation and hydrodeoxygenation to selectively remove the heteroatoms in fossil fuels since the last century [48,91]. Therefore, the commercialized sulfide catalysts (e.g., Ni, Mo and Co sulfides) are also a choice for natural oil



Table 2  
Recent studies on the deoxygenation of natural oils and related model compounds to diesel-ranged hydrocarbons over metal sulfides/phosphides/carbides.

Catalyst	Feedstock	Conditions	Solvent	Conv. (%)	Product distribution	Remarks	Ref.
NiMoS <sub>2</sub>	Palm oil	300 °C, 2 h, 30 bar H <sub>2</sub> , batch reactor	Decane	100	C <sub>14-18</sub> alkanes yield: 75.3 wt%; selectivity: n-C <sub>15</sub> = 21.8%, n-C <sub>16</sub> = 19.7%, n-C <sub>17</sub> = 29.6%, n-C <sub>18</sub> = 28.1%	Recyclability: four times	[104]
MoS <sub>2</sub>	Palmitic acid	300 °C, 50 bar H <sub>2</sub> , batch reactor	Dodecane	90	C <sub>15</sub> (C <sub>16</sub> ) hydrocarbon selectivity (%): 6 (94)		[93]
Ni <sub>3</sub> S <sub>2</sub>	Palmitic acid	300 °C, 50 bar H <sub>2</sub> , batch reactor	Dodecane	90	C <sub>15</sub> (C <sub>16</sub> ) hydrocarbon selectivity (%): 94 (6)	Apparent $E_a$ for DCO: 130 kJ mol <sup>-1</sup>	[93]
Ni-MoS <sub>2</sub>	Palmitic acid	300 °C, 50 bar H <sub>2</sub> , batch reactor	Dodecane	90	C <sub>15</sub> (C <sub>16</sub> ) hydrocarbon selectivity (%): 45 (55)	Apparent $E_a$ for DCO: 87 kJ mol <sup>-1</sup>	[93]
Sulfided ReNiMo/ $\gamma$ -Al <sub>2</sub> O <sub>3</sub>	Oleic acid	350 °C, 1 h, 40 bar H <sub>2</sub> , batch reactor	Solvent-free	100	C <sub>8</sub> -C <sub>12</sub> alkanes yield: 3.9%; C <sub>13</sub> -C <sub>18</sub> alkanes yield: 76.5%	Recyclability: six runs	[67]
Ni <sub>2</sub> P/Al <sub>2</sub> O <sub>3</sub>	Palmitic acid	300 °C, 40 bar H <sub>2</sub> , 1 h, flow reactor	Solvent-free	99.9	HDO yield: 98.8%; selectivity: C <sub>15</sub> = 75.6%, C <sub>16</sub> = 22.9%, aldehyde = 0.1%, alcohol = 0.3%, ester = 0.7%	TOF = 11.8 h <sup>-1</sup> , $E_a$ = 117 kJ mol <sup>-1</sup>	[80]
MoP/Al <sub>2</sub> O <sub>3</sub>	Palmitic acid	300 °C, 40 bar H <sub>2</sub> , 1 h, flow reactor	Solvent-free	62.8	HDO yield: 15.5%; selectivity: C <sub>15</sub> = 2.7%, C <sub>16</sub> = 22.1%, aldehyde = 6.8%, alcohol = 27.7%, ester = 0.7%	TOF = 0.2 h <sup>-1</sup> , $E_a$ = 84 kJ mol <sup>-1</sup>	[80]
Ni <sub>2</sub> P/AC	Palm oil	350 °C, 40 bar H <sub>2</sub> , 6 h, flow reactor	Solvent-free	100	Green diesel yield: 98.3%	Stable up to 6 h	[105]
NiC	Coffee oil	400 °C, 40 bar H <sub>2</sub> , 5 h, batch reactor	Solvent-free	78.9	Total liquid fuel yield: 65.3 wt%, gasoline yield: 42.0 wt%, diesel yield: 23.3 wt%		[106]
MoWC/C	Canola oil	250 °C, 450 psi H <sub>2</sub> , 2 h, batch reactor	<i>n</i> -Hexane	98	Hydrocarbon selectivity: 87.0% ( <i>n</i> -C <sub>18</sub> : 50%, <i>n</i> -C <sub>17</sub> : 34.4%)	TOF = 11.0 h <sup>-1</sup> , high activity after regeneration	[81]
Mo <sub>2.56</sub> CN <sub>0.50</sub>	Palmitic acid	300 °C, 40 bar H <sub>2</sub> , 1.2 min, fix-bed reactor	<i>n</i> -Decane	99.6	99.2% alkane selectivity, 86.0% <i>n</i> -C <sub>16</sub> selectivity		[107]

deoxygenation due to their good balance between cost, functionalities, and stability [91,92]. For the preparation of (supported) metal sulfide materials, the catalyst precursors, i.e., metal oxides, are initially obtained by thermal decomposition of the metal salts. Then, these are subjected to a thermal treatment using either a  $\text{H}_2\text{S}$  or  $\text{H}_2\text{S}/\text{H}_2$  gas mixture as a sulfurizing agent [67,93]. A summary of recent studies in the deoxygenation of natural oils and related model compounds over metal-non-metal materials is listed in Table 2. It is important to note that applying different metals in sulfide catalysts might change the selectivity of the target products by tuning the electron density of the sulfur site. Thus, the reaction can be directed toward different products depending on the metal sulfide and feedstock.

For example, Wagenhofer and coworkers studied the deoxygenation pathways of palmitic acid over  $\text{Ni}_3\text{S}_2$ ,  $\text{Mo}_2\text{S}$  and  $\text{Ni-MoS}_2$  [93]. The selectivity to  $\text{C}_{15}$  hydrocarbons (pentadecanes/pentadecenes) and  $\text{C}_{16}$  hydrocarbons (hexadecane/hexadecene) was different over  $\text{Ni}_3\text{S}_2$  and  $\text{Mo}_2\text{S}$  (see Table 2). Palmitic acid deoxygenation over  $\text{Mo}_2\text{S}$  produced hexadecane via the HDO pathway. In contrast, its deoxygenation over  $\text{Ni}_2\text{S}_3$  favored the DCO pathway to form pentadecane. Due to these singularities, the DCO pathway on  $\text{Ni}_2\text{S}_3$  and  $\text{Ni-MoS}_2$  was slightly different from that described in Fig. 1. In this case, as shown in Fig. 3, the fatty acid molecule was activated on the sulfur vacancy site of  $\text{Ni-MoS}_2$  (1  $\rightarrow$  2), subsequently forming a ketene intermediate (3) with the aid of a Mo cation and an adjacent basic sulfur atom via C-O cleavage and  $\alpha$ -proton abstraction, respectively. The carbonyl carbon interacted with the adjacent Mo cation, resulting in weakening of the C-C bond, which promoted the DCO of ketene species (3) to form  $\text{C}_{15}$  hydrocarbons. The difference in the product selectivity on  $\text{MoS}_2$  could be explained by the less basic and electron-poorer sulfur anions on  $\text{MoS}_2$  than on  $\text{Ni-MoS}_2/\text{Ni}_3\text{S}_2$ , which hampered the formation of ketene species (3).

Although a high selectivity of target products could be attained on metal sulfides, their use faces several environmental issues. For example, sulfur could leach into the reaction medium under hydrothermal conditions. This leaching might lead to the deactivation of the catalyst, decreasing its lifetime, and causing environmental pollution, as sulfur could be incorporated into the fuel liquid product/precursor.

In view of the potential environmental risks of sulfide catalysts, more attention should be paid to seeking non-sulfide catalysts for natural oil deoxygenation. Among these, metal phosphides are an environmentally-benign alternative to sulfides because they are more stable and active than sulfides in deoxygenation reactions [48,94]. Different crystal structures and metal phosphides can be synthesized during the preparation process by varying the metal to phosphorus ratio ( $x/y$  in  $\text{M}_x\text{P}_y$ ) [95,96]. This ratio is a key aspect to bear during their synthesis to control their properties and selectivity toward reaction products. In metal-rich phosphides ( $x/y \geq 1$ ), a metal phase with intensive metal-metal interactions still exists, making the properties of phosphides more similar to metals. Nevertheless, in phosphorus-rich phosphides ( $x/y < 1$ ), different metal phosphide phases exist instead of a unique metal phase [95]. For example,  $\text{Ni}_3\text{P}$ ,  $\text{Ni}_{12}\text{P}_5$ ,  $\text{Ni}_2\text{P}$ ,  $\text{Ni}_5\text{P}_4$ ,  $\text{NiP}$ ,  $\text{NiP}_2$  and  $\text{NiP}_3$  phases appear in turn by decreasing the Ni:P ratio in nickel phosphides [95]. The variation in the Ni:P ratio exhibits different activity in palmitic acid deoxygenation. Recent studies showed that increasing the Ni content to an appropriate Ni:P ratio (e.g.,  $\text{Ni}_{1.5}\text{P}$ ) gave the highest activity for deoxygenation efficiency and the highest selectivity toward pentadecane [97]. The reason for the highly active  $\text{Ni}_{1.5}\text{P}/\text{AC}$  catalyst is that the formation of an appropriate amount of  $\text{Ni}_{12}\text{P}_5$  promoted  $\text{Ni}_2\text{P}$  dispersion.

In addition, the catalytic activity and reaction pathways can also be influenced by the metal type of phosphides. Peroni et al. reported on the catalytic behavior of three types of

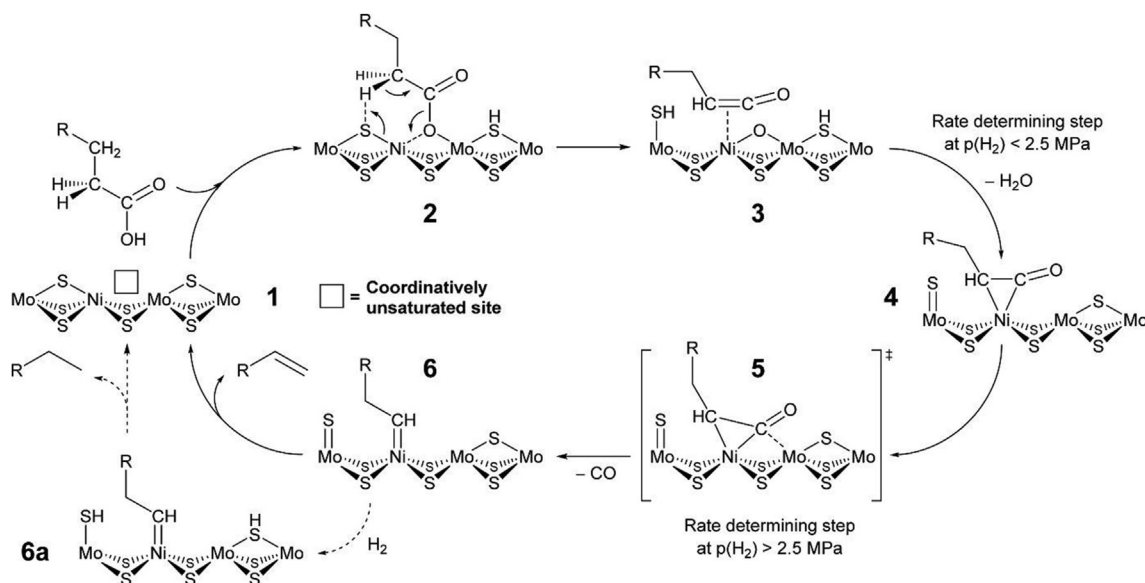


Fig. 3. Proposed decarbonylation mechanism of fatty acid on  $\text{Ni-MoS}_2$ . Reprinted with permission from ref [93]. Copyright (2017) American Chemical Society.

unsupported transition metal phosphides (Ni<sub>2</sub>P, WP, MoP) on the deoxygenation of palmitic acid [28]. It was found that palmitic acid conversion of WP and MoP favored the HDO route. Since the dehydration of hexadecanol to hexadecene requires the participation of acid sites, the selectivity to pentadecane via the DCO route was increased due to the low acidity of MoP. For Ni<sub>2</sub>P, HDO and DCO routes were both facilitated. The instinct nature of metal phosphide, i.e., metal d states density near the Fermi level of metal phosphides, as well as the acidity, influenced the bond cleavage activity (e.g., C-C cleavage) and dehydration ability, resulting in diverse selectivity to target products.

As an alternative, metal carbides also have been widely used in biomass conversion as their high activity for C-C and C-O bond cleavage is similar to that of noble metals [98]. To prepare transition metal carbides, appropriate carbon sources are required for carburization. These comprise either a solid carbon source (e.g., activated carbon and carbon nanotubes) or a gaseous carbon source (e.g., CH<sub>4</sub> and C<sub>2</sub>H<sub>6</sub>) [99,100]. Among different possible carbides, Mo<sub>2</sub>C and W<sub>2</sub>C are commonly used in deoxygenation reactions. Hollak and co-workers studied the hydrodeoxygenation of oleic acid over W<sub>2</sub>C and Mo<sub>2</sub>C catalysts [101]. In the study, carbon nanofibers were applied as the carbon source for carbide synthesis. W<sub>2</sub>C/CNF produced more olefinic products, whereas Mo<sub>2</sub>C/CNF yielded higher amounts of paraffins. Such a difference was accounted for by the faster hydrogenation rate on Mo<sub>2</sub>C/CNF. Moreover, nitrogen doping to carbon materials is also a promising alternative to enhance the catalytic activity of these materials. Introducing nitrogen to a carbon lattice could positively change its functional, chemical and electrical properties [102]. In this regard, it has been reported that the hydrotreatment activity on oleic acid was remarkably promoted by doping nitrogen into a mesoporous carbon-supported Mo<sub>2</sub>C (Mo<sub>2</sub>C/MC) catalyst. This allowed increasing the conversion from 84.8% on Mo<sub>2</sub>C/MC to 92.7% on Mo<sub>2</sub>C/N<sub>1.0</sub>MC and the hydrocarbon selectivity from 70.1% to 86.7% [103]. The formation of pyridinic and pyrrolic nitrogen increased the dispersion of Mo and promoted metal-support interactions. Both phenomena are responsible for the enhanced catalytic performance and reduced apparent *E<sub>a</sub>* over Mo<sub>2</sub>C/NMC.

These works pointed out that metal-nonmetal catalysts are active for natural oil deoxygenation, and the selectivity to DCO and HDO alkanes could be controlled by varying the active metal type. However, some issues related to sulfur leaching from metal sulfides, and relatively severe reaction conditions (250–400 °C, 30–50 bar H<sub>2</sub>) remained unsolved.

### 3.1.2. Noble metal catalysts

Noble metals (e.g., Pt, Pd and Ru) are outstandingly active and stable in catalysis due to their special d-orbital electronic configurations [108]. They have also been widely commercialized and applied in the deoxygenation of oxygenates due to their high activity for H<sub>2</sub> dissociation, reducing the energy barriers in C-O/C-C bond cleavages [109]. A summary of recent studies on noble metal-catalyzed natural oil/fatty acid deoxygenation is presented in Table 3. Among these, Pt-based

Table 3  
Recent studies on the deoxygenation of natural oils and related model compounds to diesel-ranged hydrocarbons over noble metals.

Catalyst	Feedstock	Conditions	Solvent	Conv. (%)	Product distribution	Remarks	Ref.
Pt/ZIF-67/zeolite 5 A	Palmitic acid	300 °C, 20 bar CO <sub>2</sub> , 2 h, batch reactor	Solvent-free	95	Pentadecane selectivity: 91.7%	Good recyclability	[115]
Pt/NMC	Lauric acid	300 °C, without H <sub>2</sub> , 3 h, mini-batch reactor	Tetradecane	100	<i>n</i> -Hendecane yield: 99.4%	TOF = 622 h <sup>-1</sup> , recyclability: eight cycles	[116]
Pt/TiO <sub>2</sub>	Lauric acid	30 °C, 1 bar H <sub>2</sub> , 2 h, LED irradiation (365 nm, 18 W)	Acetonitrile	>99	<i>n</i> -Hendecane yield: 93%	Recyclability: four times cyclic test	[117]
Pt/HAP-AE	Stearic acid	260 °C, 10 bar N <sub>2</sub> , 4 h, batch reactor	Deionized water	94.1	Heptadecane yield: 91.3%	Recyclability: eight runs	[110]
PtSn/SnO <sub>x</sub>	Stearic acid	320 °C, 10 bar N <sub>2</sub> , 4 h, batch reactor	<i>n</i> -Dodecane	100	Alkene yield 72.0%, alkane yield: 19.2%	Recyclability: four runs	[118]
Pt/C	Stearic acid	260 °C, 28 bar H <sub>2</sub> , 6 h, batch reactor	Cyclohexane/water (2:22) biphasic	>99	<i>n</i> -heptadecane yield: 91.7%, <i>n</i> -octadecane yield: <1.0%	Lifetime: six runs	[119]
Pt/HFA-SiO <sub>2</sub>	Soybean oil	200 °C, 10 bar H <sub>2</sub> , 24 h, batch reactor	Cyclohexane	>99	>90 wt% alkane products (C <sub>15</sub> -C <sub>18</sub> )	Effective for microbial lipid conversion	[112]
Pt@PPN	Stearic acid	150 °C, 20 bar H <sub>2</sub> , 14 h, batch reactor	Water	89.6	C <sub>17</sub> alkane selectivity: 83.5%, C <sub>18</sub> alkane selectivity: 6.1%	Recyclability: five runs	[111]
Al-modified Pd@mSiO <sub>2</sub>	Methyl palmitate	260 °C, 30 bar, 5 h, batch reactor	Cyclohexane	98%	C <sub>15</sub> selectivity: 28.1%, C <sub>16</sub> selectivity: 71.2%	Recyclability: five runs	[120]
Ru/C (ZnCl <sub>2</sub> starch)	Microalgae oil	140 °C, 50 bar H <sub>2</sub> , 6 h, batch reactor	Deionized water	100	99.6% total alkanes, 92.8% heptadecane	Recyclability: eight runs (with regeneration)	[113]
Ru <sub>1</sub> Re <sub>10</sub> /TiO <sub>2</sub>	Ethyl stearate	220 °C, 30 bar H <sub>2</sub> , 2 h, batch reactor	<i>n</i> -Hexane	99.9	<i>n</i> -C <sub>17</sub> selectivity: 22.2%, <i>n</i> -C <sub>18</sub> : selectivity: 69.7%	Recyclable for at least 5 runs	[114]
Ru/La(OH) <sub>3</sub>	Jatropha oil	240 °C, 40 bar H <sub>2</sub> , 8 h, batch reactor	<i>n</i> -Hexane	100	80.7 wt% of liquid alkane (64.8 wt% <i>n</i> -C <sub>17</sub> , 11.7 wt% <i>n</i> -C <sub>15</sub> )	Four times recyclability, 97% carbon balance	[121]
SiNA-Rh	Stearic acid	200 °C, 10 bar H <sub>2</sub> , 24 h, microwave reactor	Solvent free	NA	<i>n</i> -C <sub>17</sub> yield: 94%, <i>n</i> -C <sub>18</sub> yield: <1	Recyclability: 20 times	[122]



catalysts exhibit high natural oil deoxygenation activity and selectivity toward straight-chain DCO<sub>x</sub> alkanes. The metal-support interactions play an essential role in enhancing the activity and stability of Pt-based catalysts. Recently, Lei et al. have developed a Pt/HAP catalyst to decarboxylate natural lipid without H<sub>2</sub> effectively [110]. A considerably high yield of heptadecane was achieved under mild conditions (260 °C, 10 bar N<sub>2</sub>, 4 h), and the catalyst could be recycled at least eight times without significant loss in catalytic activity. The high activity on Pt-HAP was attributed to the interaction between PtCl<sub>6</sub><sup>2-</sup> and Ca<sup>2+</sup> from the metal and support, respectively. As a result, the reaction was synergistically catalyzed by Ca cations and Pt particles anchored by hydroxyl groups.

Additionally, Pd-based catalysts also show high activity in DCO for C<sub>n</sub> alkane synthesis. Sarkar et al. employed an efficient biobased alkane synthesis method from stearic acid with a considerable feedstock conversion (~90%) and C<sub>17</sub> alkane selectivity (83%) under extremely mild conditions (150 °C, 20 bar H<sub>2</sub>) over Pd fabricated on a Porous Organic Polymer Network (Pd@PPN) [111]. Experiments with expanded substrates proved that this catalyst was also effective for the conversion of natural oils, including palm, soybean, sunflower and rapeseed oils. Density Functional Theory (DFT) calculations showed that the interaction between Pd nanoparticles and the polymer frame structure accelerated the rate-determining step in the DCO route of stearic acid deoxygenation, which was one of the critical reasons for the high activity and selectivity of this Pd@PPN catalyst. The negative charge of Pd atoms transferred from the polymer framework played a crucial role in keeping the catalyst away from CO and unsaturated compounds poisoning, resulting in the enhanced stability and activity of Pd@PPN. Pd-based catalysts have also shown high selectivity to HDO alkanes (C<sub>n</sub> alkanes) via tuning the catalyst acidity. Liu and coworkers reported the HDO of methyl stearate and microbial lipids to produce diesel-like alkanes on hetero poly-acid-modified SiO<sub>2</sub> supported Pd (Pd/HPA-SiO<sub>2</sub>) catalysts [112]. At 200 °C, 10 bar H<sub>2</sub>, nearly a complete conversion of methyl stearate with a C<sub>18</sub> alkane yield of 76.7% was achieved. The introduction of HPA to SiO<sub>2</sub> gave extra Brønsted acid sites to the catalyst. This, together with the small Pd particles used, was responsible for the high HDO activity.

The utilization of Ru in microalgae oil hydrodeoxygenation has been investigated by Ali et al. [113]. A very high heptadecane yield (92.8%) was achieved at low reaction temperature (140 °C) over a starch-derived, mesoporous carbon, supported Ru (Ru/C) catalyst. Furthermore, designing impurity-tolerant catalysts for WCO conversion is highly desirable. Xu and coworkers synthesized a highly active Ru-HAP catalyst by an ion-exchange method to hydrogenate renewable oils to long-chain alkanes at low temperatures (full conversion at 100 °C). The Ru/HAP catalyst was also applicable for the hydrogenation of various oil sources (including jatropha oil, palm oil and WCO), and exhibited high stability (≥5 runs of recycling), with high tolerance to various impurities (e.g., salts, sugars, amino acids). The high activity and stability of Ru/HAP were due to the presence of highly dispersed Ru

nanoparticles anchored on the HAP support with fatty acids absorbed, forming a metastable calcium carboxyl phosphate [34]. In addition, several authors have reported that the modification of Ru-based catalysts with other metal(s) could lead to a change in the product selectivity. For example, Zhou et al. studied the promotion effect of the Re addition to Ru/TiO<sub>2</sub> catalysts for selective deoxygenation of ethyl stearate [114]. Without Re, the 1 wt% Ru/TiO<sub>2</sub> catalyst gave a substrate conversion of 98.4% and high selectivity toward *n*-C<sub>17</sub>H<sub>36</sub> (*n*-C<sub>18</sub>/*n*-C<sub>17</sub> = 0.5). By increasing the Re content from 0.5 wt% to 10 wt%, the ratio of *n*-C<sub>18</sub>/*n*-C<sub>17</sub> rose dramatically from 0.9 to 3.2. They reported that the addition of Re promoted the dispersion of Ru and increased the number of weak acid sites.

These noble metal catalysts have been proven highly efficient for the deoxygenation of natural oils, especially when it comes to reducing reaction temperature and pressure. Therefore, the deoxygenation process to produce alkanes can be performed under mild conditions (e.g., 140–300 °C, 0–50 bar H<sub>2</sub>). Furthermore, the deoxygenation activity and selectivity toward DCO<sub>x</sub> or HDO products could be controlled by varying the catalyst acidity and charges of the metal site via metal-support interactions. However, due to the high cost of noble metals, highly stable non-noble metal catalysts with a long lifetime against poisoning and coking are being researched.

### 3.1.3. Non-noble or base metal catalysts

Due to the environmentally-harmful presence of sulfur in metal sulfides, the high cost of noble metals and the criticality of certain noble metals, the application of non-noble or base metal catalysts in natural oil deoxygenation has received plenty of attention from researchers in recent years. Among them, Ni, Co, Cu, Mo, W have shown excellent activity within the context of biorefineries, and some of them even exhibit similar activity to noble metals [123–125]. Recent studies on natural oil/fatty acid deoxygenation over non-noble metal catalysts are summarized in Table 4. Ni-based catalysts are promising candidates due to their excellent C-C and C-O bonds cleavage performance. Jiraroj et al. reported a strategy to selectively decarboxylate biobased fatty acids in the absence of a hydrogen source over a Ni-FSM-16 catalyst [126]. After screening different active metals, including Al, Fe, Ni and Pd, they found that Ni-based catalysts exhibited the best catalytic activity, giving a high yield to linear alkanes and alkenes (up to 75%), with less than 5% of undesired cracking products. Besides, the outstanding performance of the catalysts was also attributed to the FSM-16 support. It showed abundant acidic silanol groups, which assisted the dispersion of Ni and facilitated the electron transfer from Si-Q<sup>4</sup> to Ni. As a result, this selective decarboxylation was synergistically catalyzed by the interactions between the electron-rich Ni site and the coordinating C=C in the fatty acid. This directed the carboxyl group to the silanol site for decarboxylation (Fig. 4). Ni-based catalysts also have high selectivity in the HDO for C<sub>n</sub> alkane production. Liang and coworkers studied the HDO of palmitic acid to diesel-range hydrocarbons employing a Ni/MoO<sub>2</sub>@Mo<sub>2</sub>CT<sub>x</sub> catalyst [89]. Partial oxidation of the support

Table 4  
Recent studies on the deoxygenation of natural oils and related model compounds to diesel-ranged hydrocarbons over non-noble metals.

Catalyst	Feedstock	Conditions	Solvent	Conv. (%)	Product distribution	Remarks	Ref.
Ni/palygorskite	WCO	310 °C, 40 bar H <sub>2</sub> , 9 h, batch reactor	Solvent free	100	Green diesel composition: 81.9%	Good stability of the support structure	[123]
pc-Ni/t-ZrO <sub>2</sub>	Stearic acid	240 °C, 40 bar H <sub>2</sub> , 36 h, batch reactor	<i>n</i> -Heptane	99.9	Selectivity: <i>n</i> -C <sub>17</sub> = 86.7%, <i>n</i> -C <sub>18</sub> = 5.7%, C <sub>18</sub> alcohol = 6.1%, cracking products = 1.5%	TOF = 12.4 h <sup>-1</sup>	[131]
NiW/SiO <sub>2</sub>	WCO	320 °C, 40 bar H <sub>2</sub> , 5 h, batch reactor	Solvent free	100	C <sub>17</sub> yield: 69.2%, C <sub>18</sub> yield: 30.8%	Synergy of Ni and OV site	[132]
CoNi/HAP	Methyl stearate	290 °C, methanol (transfer HDO), 10 h, batch reactor	Methanol-water	99.4	Heptadecane selectivity: 98.2%	Five times recycle; Strong electronic coupling effect of NiCo alloy	[133]
Co/t-ZrO <sub>2</sub>	Ethyl palmitate	240 °C, 20 bar H <sub>2</sub> , 8 h, batch reactor	<i>n</i> -Heptane	100	<i>n</i> -C <sub>15</sub> yield: 54.3%, <i>n</i> -C <sub>16</sub> yield: 11.9%, cracking products yield: 15.5%	TOF = 18.3 h <sup>-1</sup> , three times recyclability	[21]
Co/mix-ZrO <sub>2</sub>	Methyl laurate	240 °C, 30 bar H <sub>2</sub> , 4 h, batch reactor	<i>n</i> -Heptane	100	<i>n</i> -C <sub>11</sub> yield: 83.0%, <i>n</i> -C <sub>12</sub> yield: 8.2%, cracking products yield: 8.8%	TOF <sub>Co</sub> = 35.7 h <sup>-1</sup> , recyclability: eight runs	[134]
β-CoMoO <sub>4</sub>	Oleic acid	300 °C, 1 atm N <sub>2</sub> , 3 h, batch reactor	Solvent free	88.9	48.1% C <sub>9</sub> -C <sub>17</sub> selectivity, 69.6% oxygen removal rate	High calorific value (10, 119 cal/g), low viscosity	[124]
NiMo/Al <sub>2</sub> O <sub>3</sub>	Sunflower oil/WCO	310 °C, 40 bar H <sub>2</sub> , 9 h, semi-batch reactor	Solvent free	100	Green diesel: 97% liquid products (sunflower oil), 76% liquid products (WCO)	Stability: 200 h “time of stream”	[135]
CuNi/CoO <sub>x</sub>	Oleic acid	240 °C, isopropanol (transfer HDO), 4 h, batch reactor	Isopropanol	>99%	<i>n</i> -Heptadecane yield: 81.3%	Recyclability: five times reuse, <i>E<sub>a</sub></i> = 91.52 kJ mol <sup>-1</sup>	[130]
CuNi/ZrO <sub>2</sub>	Oleic acid	370 °C, methanol (transfer HDO), 5 h, batch reactor	Methanol-water	100	92.5% heptadecane selectivity	Recyclability: three times	[136]
CuNi <sub>2</sub> Al	Oleic acid	330 °C, methanol (transfer HDO), 5 h, batch reactor	Methanol-water	100	92.7% heptadecane selectivity	Cu-Ni alloy inhibits the C-C cracking	[137]
Ni-Fe/γ-Al <sub>2</sub> O <sub>3</sub> or HZSM-5	Palmitic acid	270 °C, 15 bar H <sub>2</sub> , 6 h, semi-batch reactor	Cyclohexane	100	Selectivity: <i>n</i> -C <sub>15</sub> 72.2%, <i>n</i> -C <sub>16</sub> 11.5% (Ni-Fe/γ-Al <sub>2</sub> O <sub>3</sub> ); <i>n</i> -C <sub>15</sub> 8.3%, <i>n</i> -C <sub>16</sub> 60.5% (Ni-Fe/HZSM-5)	Bimetallic Ni-Fe exhibits good coke resistance	[138]
Co <sub>3</sub> O <sub>4</sub> /SiO <sub>2</sub> -Al <sub>2</sub> O <sub>3</sub>	Jatropha oil	250 °C, 30 bar H <sub>2</sub> , 6 h, batch reactor	Hexadecane	100	Yield of liquid hydrocarbon: 73.8 wt%	Recyclability: three cycles	[139]

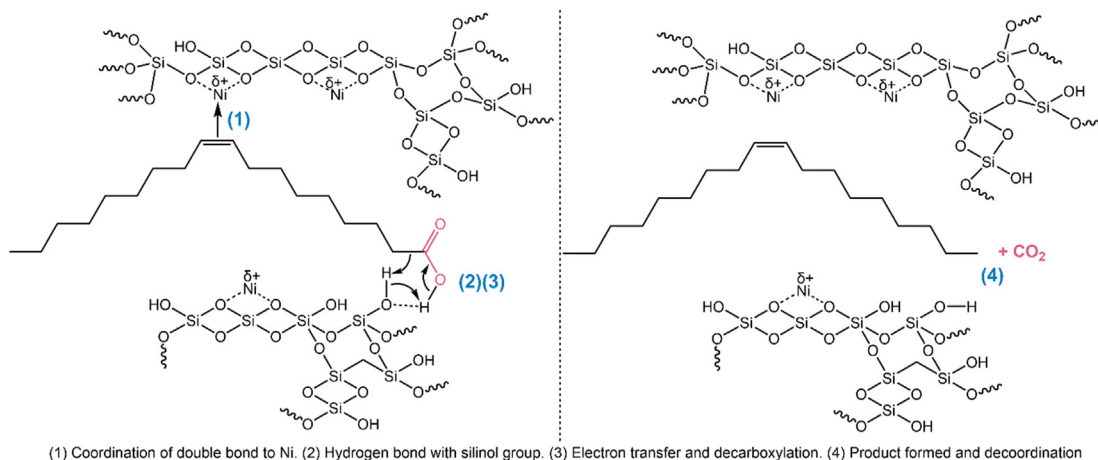


Fig. 4. Oleic acid decarboxylation mechanism on Ni-FSM-16 catalyst. Reprinted with permission from ref [126]. Copyright (2021) Elsevier.

Mo<sub>2</sub>CT<sub>x</sub> Mxene was conducted to enhance the HDO activity and reduce carbon loss. As a result, a higher C<sub>16</sub>/C<sub>15</sub> alkane ratio was obtained over the Ni/MoO<sub>2</sub>@Mo<sub>2</sub>CT<sub>x</sub> catalyst than with pure Ni. These results showed that the MoO<sub>2</sub> active site played a crucial role in promoting the dehydration-hydrogenation route.

Alternatively, Co-based catalysts have also shown high activity in the deoxygenation of natural oils. A high atom-economical HDO selectivity to fuel products can be produced over Co catalysts. Soni et al. applied a Co<sub>3</sub>O<sub>4</sub>/silica-alumina as a catalyst in the deoxygenation of methyl stearate and a natural oil feedstock [127]. A complete conversion (100%) and high HDO products selectivity (87%) was achieved on the 6 wt% Co<sub>3</sub>O<sub>4</sub>/SiO<sub>2</sub>-Al<sub>2</sub>O<sub>3</sub> catalyst under relatively mild conditions (250 °C, 30 bar H<sub>2</sub>, 6 h) from the deoxygenation of methyl stearate. By increasing the reaction temperature to 300 °C, a relatively higher ratio of cracking products was observed. In addition, the application of bimetallic catalysts in fatty acid deoxygenation showed tunable selectivity toward DCO<sub>x</sub> or HDO product by varying the ratio of metals, and thereby the fuel properties can be controlled. Soni and co-workers developed green Ni/Co-natural clay catalysts for the selective conversion of microalgae oil to green diesel [128]. During the hydrotreatment of methyl oleate, the Ni/clay showed a high selectivity to *n*-heptadecane (88%). The Co/clay was selective for *n*-octadecane production (90%), and the Ni/Co bimetallic catalysts were suitable to produce diesel fuel containing both *n*-heptadecane and *n*-octadecane. These catalysts were also reactive and stable enough to be applied in microalgae oil hydroprocessing.

Other non-noble or base metals, such as Mo, Cu, Fe and W, can also be applied in deoxygenation reactions. However, the deoxygenation of natural oils over these metals shows low conversion/products yield, and needs to be conducted under severe conditions. A common approach to this challenge is the use of bi-metallic catalysts. These exhibit higher activity/selectivity than monometallic catalysts under the same reaction conditions [124,125,129]. The less active metal is usually used as a promoter in bimetallic catalysts to enhance the

catalyst properties, such as electron distribution, metal dispersion, surface acidity/basicity, of its counterpart. Based on this approach, Zhong et al. developed a solvent- and hydrogen-free stearic acid deoxygenation process using a graphitic carbon embedded Fe-Ni catalyst [88]. They found that varying the carburization temperature led to a change in the thickness of the carbon shell and the size of the Fe-Ni alloy core. Consequently, the catalytic activity over a Fe-Ni@C-800 catalyst was significantly improved compared with those achieved with Fe/C, Ni/C, and Fe-Ni/SiO<sub>2</sub> catalysts. The bimetallic catalysts completed a 99.9% substrate conversion with 76.8% heptadecane selectivity. Wang and coworkers developed a bifunctional and magnetically recoverable CuNi/CoO<sub>x</sub> catalyst for the hydrogenation of oleic acid to *n*-heptadecane [130]. This Cu<sub>1</sub>Ni<sub>1</sub>/CoO<sub>x</sub> exhibited enhanced catalytic performance compared with Ni/CoO<sub>x</sub>, with >99% conversion and 91.3% *n*-heptadecane yield at 240 °C in 8 h, using isopropanol as a hydrogen source.

Overall, non-noble or base metal catalysts are cheaper than noble metals but exhibit lower catalytic performance under relatively severe reaction conditions (240–320 °C, 0–40 bar H<sub>2</sub>). Nickel is more active in C-C bond cleavage, whereas Co tends to be more selective toward HDO products. In addition, introducing other transition metals as a promoter shows an enhanced activity and a change/reverse in selectivity. As an alternative to noble metals, more efficient and stable base metal catalysts should be designed to achieve the right balance between energy consumption and the cost of raw materials.

### 3.2. Jet-ranged hydrocarbons

Jet fuel must meet some standards for fuel quality to prolong the engine lifetime and avoid the generation of harmful exhaust gases [140]. The international standard for pure and/or blended bio-jet (ASTM D7566) should meet the following properties: aromatics, 8–25 vol%; sulfur, 0.0325 wt%; heat of combustion >42.8 MJ kg<sup>-1</sup>; freezing point, -47 °C; flash point >38 °C; density, 0.775–0.840 kg/L; acid no. < 0.1 mg of

KOH/g [47]. To satisfy these standards, jet fuel components should be branched C<sub>10</sub>-C<sub>12</sub> paraffins, cycloparaffins and/or multi-branched C<sub>13</sub>-C<sub>16</sub> paraffins [140]. Therefore, to obtain jet-ranged hydrocarbons, the formed linear alkanes via the DCO<sub>x</sub> and HDO reactions from the conversion of natural oils should be further hydroprocessed by hydrocracking, isomerization and aromatization to produce a mixture of hydrocarbons (Fig. 1). For these steps, catalysts with abundant acidic sites are required because the isomerization and cracking reactions usually occur on these, generating carbocations as the key intermediates (Fig. 5) [20,49,141]. Therefore, the catalysts mentioned above for diesel fuel synthesis might not be suitable for bio-jet fuel production, and some bifunctional/multifunctional catalysts with activity in isomerization, cracking and aromatization should be designed.

Table 5 lists recent work on bio-jet fuel production from natural oil feedstocks. Commonly, zeolite-based catalysts (e.g., HZSM-5, SAPO-11 and Y zeolite supported metal catalysts) are widely applied in the hydrocracking process due to their high concentration and strength of acid sites, which are beneficial for cracking and isomerization reactions [77,142–144]. It has been reported that medium acid sites facilitate cracking, while strong acid sites promote isomerization [47,145]. Therefore, it is possible to experimentally control the selectivity of specific hydrocarbon products by varying the acidity of the catalysts.

The hydroprocessing of natural oil could be a multi-step process, including an initial deoxygenation reaction yielding liquid linear alkanes over one type of catalyst, and a subsequent cracking/isomerization of the paraffin products using another catalyst. Finally, distillation is required to fractionate the jet-ranged fuel from the product mixtures (Fig. 6) [42,146]. Recently, Jeong et al. developed a Pt/mesoporous  $\gamma$ -Al<sub>2</sub>O<sub>3</sub> (MA) catalyst with excellent stability combined with Pt/Y for bio-jet fuel synthesis [29]. The Pt/MA catalyst gave an alkane yield of 83% and superior stability for more than 100 h. The resulting alkanes were hydrocracked over a Pt/zeolite Y, forming 81.6 wt% of liquid products with the *iso* to *n*-paraffin ratio of 4.67:1. The final fuel product obtained from distillation met the ASTM standards. Furthermore, maximizing the bio-jet fuel yield is crucial during the hydrocracking process. Kim et al. developed a strategy for maximizing the bio-jet fuel yields by a two-step deoxygenation/hydrocracking process [141]. Compared with the single-step process, the two-step deoxygenation-hydrocracking exhibited a higher yield of bio-jet fuel, lower aromatic content and longer catalyst lifetime. By

suppressing over-cracking, a bio-jet fuel yield as high as 55 wt % (satisfy ASTM D7566-14 standard) was achieved using a nanocrystalline large-pore zeolite beta supported Pt catalyst.

Despite these promising features, the multi-step processes might cause some inconvenience and extra energy consumption. Therefore, developing multifunctional catalysts for one-step bio-jet fuel synthesis has attracted the attention of researchers worldwide. However, the carbon monoxide formed during the deoxygenation reaction might poison metal-based catalysts and decrease their lifetimes. Additionally, over-cracking to light alkanes in the gaseous phase is an issue that must be overcome [141,146]. To solve this, Lee and coworkers studied the bio-jet fuel synthesis via a one-step hydroconversion of triglycerides over a Pt-Re supported on an ultra-stable Y catalyst with CO-tolerant ability [146]. With the addition of Re, poisoning by CO could be successfully suppressed by weakening the interaction of the catalyst with CO and rapidly converting CO into CH<sub>4</sub>. As a result, a one-step process with negligible coke formation could obtain a high-quality bio-jet fuel yield of 41 wt%.

Notwithstanding these promising results, bio-jet fuel production from natural oils must be performed at relatively high temperatures (240–450 °C), resulting in increased energy consumption. Therefore, efforts are still needed to develop more efficient catalytic systems for bio-jet fuel synthesis from natural oils to find an appropriate balance between the cost and profit. In addition, cracking reactions occur during synthesizing bio-jet fuel, resulting in a significant carbon loss. Thus, it is important to find a method to directly synthesize branched or cyclic hydrocarbons rather than the classical two-step deoxygenation/isomerization process.

#### 4. Fatty alcohols production

Based on the biorefinery concept, the synthesis of valuable products and biofuels from natural oil deoxygenation should be considered to fulfill different present and future market needs. Fatty alcohols, another potential product from the partial deoxygenation of natural oils, are of high value as key intermediates to manufacturing household detergents, cosmetics and other industrial chemicals [45,46,154]. Traditionally, Cu-Cr-based catalysts have been applied to produce fatty alcohols from fatty acids/natural oils hydrogenation [155]. However, the potential environmental issues caused by Cr leaching and the severe reaction conditions make the catalysts and process less attractive [156].

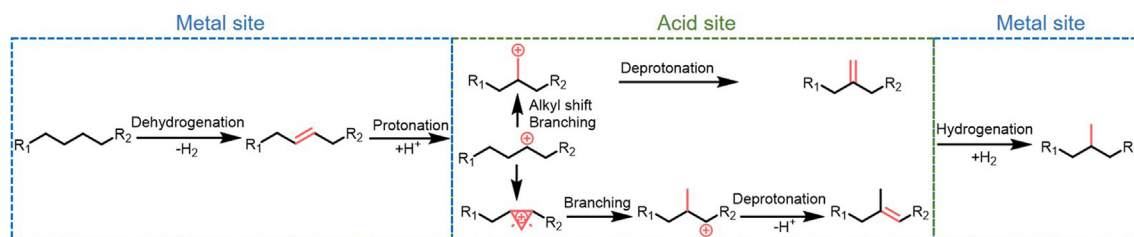


Fig. 5. Hydrocracking and isomerization mechanism of *n*-alkane to branched alkane.

Table 5  
Recent studies on bio-jet fuel synthesis from natural oils.

Catalyst	Feedstock	Conditions	Solvent	Product distribution	Remarks	Ref.
NiMo sulfide/ZnZSN-5/ $\gamma$ -Al <sub>2</sub> O <sub>3</sub>	Methyl oleate	450 °C, 5 bar H <sub>2</sub> , WHSV = 6.1 h <sup>-1</sup> , fixed bed flow reactor	Solvent free	Aromatics yield: 20 wt%, <i>iso</i> -/ <i>n</i> -(C <sub>5</sub> -C <sub>14</sub> ) = 4.4, selectivity: gas (C <sub>1</sub> -C <sub>4</sub> ) = 33%, gasoline (C <sub>5</sub> -C <sub>11</sub> ) = 47%, kerosene (C <sub>12</sub> -C <sub>14</sub> ) = 47%, diesel (C <sub>15</sub> -C <sub>18</sub> ) = 7.5%, C <sub>19</sub> = 4.9%		[147]
Ni-MoS <sub>2</sub> / $\gamma$ -Al <sub>2</sub> O <sub>3</sub>	Palm kernel oil	330 °C, 50 bar H <sub>2</sub> , LHSV = 1 h <sup>-1</sup> , continuous bed reactor	Solvent free	58% selectivity of C <sub>10</sub> -C <sub>12</sub> hydrocarbons, ~92% yield of products		[148]
Ni <sub>2</sub> P/Zr-SBA-15	Jatropha oil	330 °C, 45 bar H <sub>2</sub> , 4 h, batch reactor	Solvent free	79.25 wt% paraffins, 10.13 wt% aromatics, 6.72 wt% naphthene	Meeting ASTM-D7566-2017b standard	[149]
Pt/mesoporous $\gamma$ -Al <sub>2</sub> O <sub>3</sub> and Pt/Y	Palm oil	380 °C, 40 bar H <sub>2</sub> , WHSV = 2.5 h <sup>-1</sup> , down-flow trickle-bed reactor; ~240 °C, 50 bar H <sub>2</sub> , WHSV = 2 h <sup>-1</sup>	Solvent free	Yield of hydrocarbon products: 83 wt%, <i>iso</i> -/ <i>n</i> -paraffin = 0.05; C <sub>8</sub> -C <sub>16</sub> selectivity: 66.1 wt%, <i>iso</i> -/ <i>n</i> -paraffin = 6.25	More than 100 h lifetime, meeting the bio-jet fuel standards	[29]
PtRe/USY	Palm oil	295 °C, 40 bar H <sub>2</sub> , WHSV = 2.0 h <sup>-1</sup> , down-flow plug-flow reactor	Solvent free	Jet fuel yield: 41 wt%, <i>iso</i> -/ <i>n</i> -paraffin = 5.1	Net heat of combustion: 46.9 MJ kg <sup>-1</sup> , meet the jet fuel standard	[146]
Pd/C	Palm kernel oil	400 °C, N <sub>2</sub> , 2 h, continuous reactor	Solvent free	~96% yield of liquid product, 73% jet paraffin selectivity	Blending with Jet A-1 meets ASTM standards	[150]
NiO-LiZSM-5	Waste oils	360 °C, 40 bar H <sub>2</sub> , 6 h, batch reactor	Solvent free	91.7% jet fuel content (80.42% jet fuel from oleic acid conversion, 3.72% <i>n</i> -paraffins, 39.36% <i>i</i> /cycle-paraffins, 37.34 arenes)		[49]
PtNi/NH <sub>4</sub> -Beta	Palm olein	360 °C, 40 bar H <sub>2</sub> , 4 h, batch reactor	Solvent free	Bio-jet yield: 28.7%, <i>iso</i> -/ <i>n</i> -alkane ratio: 1.02	The bio-jet could be blended with Jet A-1 to meet ASTM standard	[151]
Mo/HZSM-22	Palmitic acid	260 °C, 40 bar H <sub>2</sub> , 4 h, batch reactor	<i>n</i> -Decane	Selectivity: 100% alkanes, 3.2% <i>n</i> -C <sub>14</sub> , 7.5% <i>n</i> -C <sub>15</sub> , 30.3% multi. <i>Iso</i> -C <sub>16</sub> , 31.4% mono. <i>Iso</i> -C <sub>16</sub> , 27.4% <i>n</i> -C <sub>16</sub>		[152]
NiAg/SAPO-11	Palm oil	360 °C, 30 bar H <sub>2</sub> , LHSV = 1 h <sup>-1</sup> , fixed bed reactor	Solvent free	Aromatics content: 9.0%, <i>i</i> -/ <i>n</i> -alkane: 1.5, liquid product yield: 55.6%	Meeting jet fuel specifications	[153]



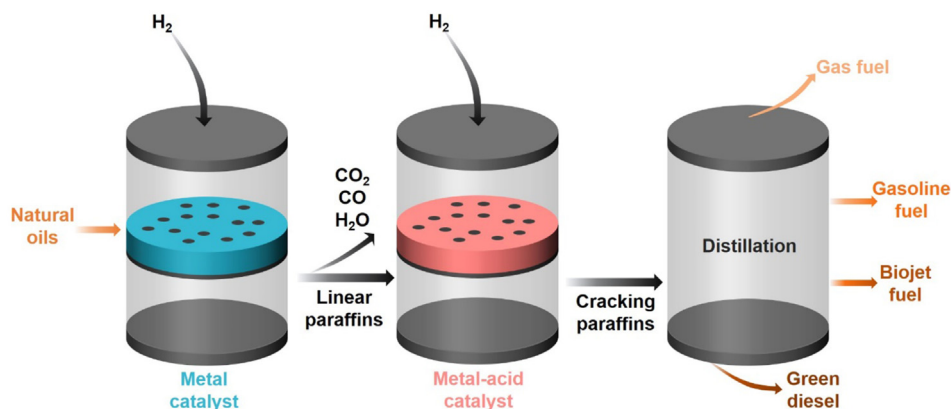


Fig. 6. Process of natural oil conversion to bio-jet fuel.

Therefore, developing alternative environmentally friendly and highly active catalysts are urgently required. Additionally, fatty alcohols can be divided into saturated and unsaturated. Saturated fatty alcohols can be obtained from the hydrogenation of both unsaturated and saturated fatty acids, whereas unsaturated fatty alcohols could only be synthesized by the selective hydrogenation of the carboxylic group with C=C bonds unchanged. Compared with saturated alcohols, unsaturated fatty alcohols have outstanding advantages. These include lower melting points, better water solubility and, more importantly, the capability of introducing other functional groups into their structure [45]. This section critically reviews and discusses the production of unsaturated/saturated fatty alcohols from the hydrogenation of natural oil or related model compounds over heterogeneous catalysts.

#### 4.1. Unsaturated fatty alcohols

Regarding the production of unsaturated fatty alcohols, oleic acid or methyl oleate are usually used as the feedstock, with oleyl alcohol being the target product [157,158]. The catalysts used in this process should have high activity and selectivity on the hydrogenation of the carboxylic group to the hydroxyl group, without losing the unsaturation of the aliphatic chain. In these processes, Ru-, Rh- and Co-based catalysts show outstanding activity and selectivity toward oleyl alcohol [74,156,159] (Table 6). The hydrogenation rate of the C=C bond is usually faster than that of the C=O bond over monometallic catalysts (e.g., Ru, Rh and Co) [160]. However, introducing modifiers or promoters such as tin and/or boron to the catalysts can selectively modulate the activity toward C=C bond hydrogenation [74,158,160]. In this respect, Vigier et al. developed a strategy for the methyl oleate hydrogenation to oleyl alcohol using CoSn/ZnO catalysts with high efficiency [159]. It was found that Co-Sn<sub>2</sub> particles were the active phase for methyl oleate hydrogenation into oleyl alcohol, and the amount of active phase could be increased by varying the metal precursors. The maximum selectivity to oleyl alcohol could be as high as 55%, with 80% methyl laurate conversion over the CoSn/ZnO catalyst when Co(CO)<sub>8</sub> was used as the precursor. Moreover, Ru-Sn-B and Rh-Sn-B

catalysts are usually applied in oleyl alcohol production from oleic acid/methyl oleate. Benítez and coworkers investigated the influence of Sn content in Rh-Sn-B/Al<sub>2</sub>O<sub>3</sub> catalysts on the selective hydrogenation of oleic acid to fatty alcohols [161]. They found that the yield of oleyl alcohol increased with the rise of Sn content from 1 wt% to 5 wt%, and an oleyl alcohol yield as high as 85.5% could be achieved over the Ru<sub>1</sub>Sn<sub>4</sub> and Ru<sub>1</sub>Sn<sub>5</sub> catalysts. In these formulations, Sn acted as a promoter for limiting the Rh activity on C=C bond saturation by forming Rh-SnO<sub>x</sub> species, which were also the active phase for C=O hydrogenation. Sánchez et al. studied the effect of the support (Al<sub>2</sub>O<sub>3</sub>, SiO<sub>2</sub> and TiO<sub>2</sub>) on Ru-Sn-B catalysts during the selective hydrogenation of methyl oleate to oleyl alcohol [160]. Their experimental results suggested that the support significantly influenced the Ru particle size and the interactions between Ru and Sn, which resulted in different catalytic activity and product selectivity. Among the tested catalysts, Ru-Sn-B/Al<sub>2</sub>O<sub>3</sub> was the best for oleyl alcohol production, whereas a high yield of stearyl alcohol was obtained over Ru-Sn-B/SiO<sub>2</sub>. However, the Ru-Sn-B/TiO<sub>2</sub> catalyst favored C=C bond hydrogenation but had low activity in hydrogenating the C=O bond, leading to a high selectivity to methyl stearate.

These findings show that the main challenge in oleyl alcohol production from oleic acid/methyl oleate is the relatively low yield/selectivity of oleyl alcohol and the formation of other by-products or undesired intermediate products [162], such as stearyl alcohol and alkanes, from over-hydrogenation and heavy esters from transesterification. Therefore, efforts should be directed toward designing efficient catalysts with high activity in the selective hydrogenation of the C=O bond without promoting the C=C bond saturation.

#### 4.2. Saturated fatty alcohols

The selection of catalysts and substrates for synthesizing saturated fatty alcohols is more flexible than that for synthesizing unsaturated fatty alcohols. This accounts for the fact that there is no need to protect the unsaturation in the carbon chain. The critical point for obtaining saturated fatty alcohols is to suppress the excessive deoxygenation to hydrocarbons

and/or their transesterification to heavy esters. Lower reaction temperatures are usually required compared to the alkane synthesis because of the higher energy barriers in the DCO and HDO reactions than during the hydrogenation to alcohols [21,28,134,164,165]. Table 7 summarizes the catalysts and operation details for synthesizing saturated alcohols from natural oils and related model compounds. A wide variety of catalysts can be applied in the process, including both noble and non-noble metals.

As mentioned in the previous sections, noble metals are highly active for C-C and C-O bond cleavages, resulting in an excellent performance in the deoxygenation of natural oils. However, some noble metal catalysts (e.g., Pt and Rh) resulted in low selectivity to fatty alcohols due to their high C-C cleavage rate [46]. In addition to these, Pd, Ru and Re are found to have the capability of yielding fatty alcohols with high selectivity from the hydrogenation of natural oils or related model compounds [164,166,167]. Guo et al. developed a Pd stabilized Cu-Zn-Al catalyst for the selective hydrogenation of natural oils to alcohols or alkanes [165]. Under mild conditions (200 °C and 2 MPa), the catalyst yielded nearly 100% of *n*-decanol, whereas 100% of decanes (including *n*- and *i*-decane) were obtained by adding HZSM-5 as a solid acid. Cu species were the active center, and Pd helped stabilize the catalyst from Cu leaching. Ru-Sn catalysts are promising and commonly used candidates for synthesizing fatty alcohols. Luo and coworkers found that the active sites in the selective hydrogenation of fatty acids to fatty alcohols in a Ru-Sn/SiO<sub>2</sub> catalyst were Ru<sub>3</sub>Sn<sub>7</sub> nano-clusters [27]. Based on XPS analysis, the shifts in binding energies of metallic Ru and Sn showed that a Ru<sub>3</sub>Sn<sub>7</sub> alloy was formed instead of Ru-SnO<sub>x</sub> species. When the Ru/Sn ratio was lower than 3/7, an excess in SnO<sub>2</sub> or Sn caused the formation of undesired ester as an intermediate product. The DFT calculations revealed that the energy barrier for the rate-determining step catalyzed by Ru<sub>3</sub>Sn<sub>7</sub> (111) was lower than that catalyzed by Ru (0001). In addition, the ReO<sub>x</sub> species or their combination with noble metals are extraordinarily efficient in carboxylic acid hydrogenation. Ali et al. reported a strategy using a 4% ReO<sub>x</sub>/TiO<sub>2</sub> solid as the catalyst for the hydrogenation of fatty acids to alcohols [168]. The highest selectivity to octadecanol reached 93% at mild conditions (180–200 °C and 2–4 MPa).

Developing low-cost, non-noble metal catalysts for fatty alcohols production from natural oils is also a promising research area. Supported Ni catalysts are highly active in the HDO of natural oils, but their high activity in C-C cleavage results in low selectivity toward fatty alcohols. Recent studies have reported that modifying Ni with another metal/metal oxide (e.g., Fe, Cu, VO<sub>x</sub>, MoO<sub>x</sub>) can enhance fatty alcohol selectivity [169–171]. Kong et al. employed a carbon-coated Ni-Fe catalyst for the selective hydrogenation of stearic acid [172]. Over the optimal catalyst, Ni1.8Fe1.5, almost full conversion (>99%) and high selectivity (~98%) were achieved under the optimal reaction conditions. As proven by DFT calculations, the affinity of iron sites with the -COOH groups and the dissociation of H<sub>2</sub> on nickel sites were

Table 6  
Recent studies on unsaturated fatty alcohol synthesis from the hydrogenation natural oils and model compounds.

Catalyst	Feedstock	Conditions	Solvent	Conv. (%)	Product distribution	Remarks	Ref.
CoSn/ZnO	Methyl oleate	270 °C, 80 bar H <sub>2</sub> , 21 h, batch reactor	Solvent free	80	55% selectivity to unsaturated alcohol	Co-Sn <sub>2</sub> as the active species	[159]
RuSnB/Al <sub>2</sub> O <sub>3</sub>	Oleic acid	290 °C, 50 bar H <sub>2</sub> , 1 h, batch reactor	n-Dodecane	89.27	44.71% selectivity to oleyl alcohol	The loss of active material results in catalyst deactivation	[157]
CoSnB/Al <sub>2</sub> O <sub>3</sub>	Methyl oleate	270 °C, 40 bar H <sub>2</sub> , 5 h, batch reactor	Solvent free	75	49.5% selectivity to unsaturated alcohol		[163]
CoSn/Al <sub>2</sub> O <sub>3</sub> -sol-gel	Methyl oleate	270 °C, 80 bar H <sub>2</sub> , 36 h, batch reactor	Solvent free	80	62% selectivity to unsaturated alcohol		[163]
RhSnB-Al <sub>2</sub> O <sub>3</sub>	Oleic acid	270 °C, 50.7 bar H <sub>2</sub> , 2 h, batch reactor	Dodecane	100	85.5% yield of oleyl alcohol	Rh-SnO <sub>x</sub> species are the active sites for C=O hydrogenation	[161]
RhSnB/Al <sub>2</sub> O <sub>3</sub>	Oleic acid	270 °C, 20 bar H <sub>2</sub> , 200 min, batch reactor	Dodecane	100	85% yield of oleyl alcohol	Pairwise insertion of hydrogen to the fatty molecule is the rate-limiting surface reaction step	[74]

Table 7  
Recent studies on saturated fatty alcohol synthesis from the hydrogenation natural oils and model compounds.

Catalyst	Feedstock	Conditions	Solvent	Conv. (%)	Product distribution	Remarks	Ref.
Pd/Re/C	Stearic acid	130 °C, 20 bar H <sub>2</sub> , 18 h, batch reactor	<i>n</i> -Hexane	100	87% octadecanol selectivity, traces of alkanes	Also capable of preparing alkanes	[164]
Pd/CuZnAl	Coconut oil	200 °C, 20 bar H <sub>2</sub> , 18 h, batch reactor	<i>n</i> -Octane	100	80.2% yield of fatty alcohols	Also capable of preparing alkanes, recyclability of five times	[165]
Ru/NH <sub>2</sub> -rGO	Palmitic acid	210 °C, 100 bar H <sub>2</sub> , 22 h, batch reactor	1,4-Dioxane	>99	93% yield of aliphatic alcohol	Four times of reusability	[167]
RuSn/N-C	Algae oil	140 °C, 50 bar H <sub>2</sub> , 6 h, batch reactor	Water	100	100% yield of fatty alcohols	Eight recycles without significant activity loss	[168]
ReO <sub>x</sub> /TiO <sub>2</sub>	Stearic acid	200 °C, 40 bar H <sub>2</sub> , batch reactor	Dodecane	100	93% octadecanol selectivity, <7% alkanes		[174]
Cu/SiO <sub>2</sub>	Coconut oil	240 °C, methanol (transfer hydrogenation), 4 h, batch reactor	Methanol	85	100% selectivity to fatty alcohols	Synergistically catalyzed by Cu <sub>2</sub> O-SiO <sub>2</sub> and Cu <sup>0</sup>	[175]
CuZn <sub>x</sub> @C	Methyl laurate	200 °C, 80 bar H <sub>2</sub> , 72 h, batch reactor	<i>n</i> -Hexane	81.3	77% selectivity to fatty alcohol	Cu-O-Zn as the active site, recyclability: three times	[176]
Magnetic recoverable Co	Oleic acid	200 °C, isopropanol (transfer hydrogenation), 4 h, batch reactor	Isopropanol	100	91.9% octadecanol selectivity	Active species: Co <sup>0</sup> and Co <sup>δ+</sup> , ten times of reusability	[173]
Cobalt oxide	Stearic acid	200 °C, 20 bar H <sub>2</sub> , 3 h, batch reactor	Alkane solvent	100	98.3% fatty alcohol selectivity	Cobalt monoxide as the active phase	[177]
Co/HAP	Methyl stearate	200 °C, methanol (transfer hydrogenation), 5 h, batch reactor	<i>n</i> -hexane	94.8	67.7 octadecanol selectivity	Five times of reusability	[178]
CuCo/C	Lauric acid	330 °C, methanol (transfer HDO), 3 h, batch reactor	Methanol-water	79	62.3 yield of lauryl alcohol	Three times recyclability	[179]
Ni-In/SiO <sub>2</sub>	Methyl octanoate	270 °C, 35 bar H <sub>2</sub> , 4 h <sup>-1</sup> WHSV, fixed-bed reactor	Cyclohexane	98.4	95.2% fatty alcohol selectivity	240 h of lifetime	[72]
Ni-VO <sub>x</sub> /TiO <sub>2</sub>	Methyl palmitate	220 °C, 40 bar H <sub>2</sub> , 7.5 h, batch reactor	Cyclohexane	>99	90% cetyl alcohol selectivity	Ternary synergistic effect of Ni, OV and Lewis acid sites	[171]
Ni-MoO <sub>x</sub> /CeO <sub>2</sub>	Stearic acid	235 °C, 30 bar H <sub>2</sub> , 3 h, batch reactor	Cyclohexane	98	96.2% octadecanol selectivity	Synergistic catalysis sites of electron-deficient Ni and MoO <sub>x</sub>	[170]

responsible for the high selectivity to fatty alcohols (Fig. 7). The Ni-Fe catalyst also exhibited high stability and could be recycled for at least five runs. Han and coworkers designed a Ni-Fe alloy oxide catalyst to selectively synthesize fatty alcohol from fatty acid hydrodeoxygenation [169]. During the reaction, the excessive deoxygenation to alkane is suppressed by introducing lattice oxygen via over oxidation of Ni-Fe alloy. This leads to the formation of a more stable  $\eta^2(\text{C}, \text{O})$ -aldehyde adsorption configuration rather than  $\eta^1(\text{C})$ -acyl. As a result, 90% selectivity to lauryl alcohol was achieved with 100% conversion. In addition, Cu-based catalysts are promising candidates for transforming renewable fatty acids into valuable fatty alcohols. Zhang et al. studied the role of the  $\text{ZrO}_2$  crystal structure and metal-support interface of Cu/ $\text{ZrO}_2$  catalyst on the transfer hydrogenation of lauric acid with methanol as the hydrogen source [70]. It was found that the as-prepared Cu/tetragonal- $\text{ZrO}_2$  (Cu/t- $\text{ZrO}_2$ ) catalyst exhibited superior activity than a Cu/monoclinic- $\text{ZrO}_2$  (Cu/m- $\text{ZrO}_2$ ) catalyst during the hydrogenation of lauric acid. The DFT calculations and catalyst characterization results showed that the better catalytic performance of the Cu/t- $\text{ZrO}_2$  was caused by its higher amount of oxygen vacancies and abundant metal-support interface. The metal-support interface was responsible for promoting the C-O cleavage and  $\text{H}_2$  dissociation, resulting in a decrease in the energy barrier of the reaction. In addition to Ni and Cu, Co, as the active metal, can also be applied in fatty alcohols production. Several studies have reported that the active species of Co-based catalysts for fatty acid hydrogenation are not only metallic cobalt but also cobalt oxides or  $\text{Co}^{\delta+}$  species. Wang and coworkers developed a magnetically recoverable Co catalyst for the catalytic transfer hydrogenation of oleic acid to octadecanol using isopropanol as a hydrogen source [173]. They found that the optimal catalyst contained partially reduced Co, resulting in an octadecanol yield of 91.9%. The characterization of the catalyst showed that  $\text{Co}^0$  and  $\text{Co}^{\delta+}$  were present on the catalyst surface, with both acting as the active center for oleic acid hydrogenation. In addition to this outstanding catalytic activity, the as-synthesized Co catalyst could be recycled ten times via magnetic recovery.

These publications showed that noble and non-noble metals are efficient for value-added fatty alcohols production from the

hydrogenation of natural oils or renewable fatty acids/esters. However, the main issue in the conversion process is to avoid the formation of heavy esters and/or alkanes. It is reported in the literature that the presence of acid and base sites on the catalyst surface promotes the formation of heavy esters, and the proper increase in the reaction temperature favors the formation of alkanes [20,134]. To solve this, it is feasible and highly desirable to design catalysts with proper acidity and basicity, adding promoters to suppress alkane formation and decrease the reaction temperature.

## 5. Controlling the products selectivity

Designing appropriate catalytic systems with tunable selectivity to synthesize value-added fatty alcohols or hydrocarbons (diesel-range) for energy usage is exceptionally beneficial for achieving a holistic “natural oil biorefinery”. During natural oil deoxygenation, the formation of fatty alcohol intermediates and their further deoxygenation to alkanes are tandem reactions [58,180]. To achieve a reasonable control of the process, it is vital to select the reaction conditions properly (e.g., temperature, time, pressure), carefully adjust the properties of the catalysts (e.g., metal type, acidity, basicity, metal-support interface, and electron properties), and use promoters and/or additives to increase the efficiency of the reaction systems [72,128,131,134,165]. Table 8 summarizes the characteristics of active metal, support and metal support interactions and their influences on natural oils deoxygenation. A diagram summarizing recent studies addressing the deoxygenation of fatty acids/esters to alkanes or alcohols with tunable selectivity is depicted in Fig. 8. This section summarizes and critically discusses the factors influencing the selectivity toward target products.

Based on many recent kinetic studies covering the fatty acid deoxygenation, the activation energy of fatty acids hydrogenation to alcohols is much higher than those of alcohols/aldehydes deoxygenation (i.e., DCO or HDO) to alkanes. Additionally, the activation energies of hydrocracking, isomerization are even higher than DCO and HDO [134,181]. Therefore, the reaction temperatures required for synthesizing potential target products are as follows: fatty alcohols < diesel-ranged hydrocarbons < jet-ranged hydrocarbons. For synthesizing fatty alcohols, the

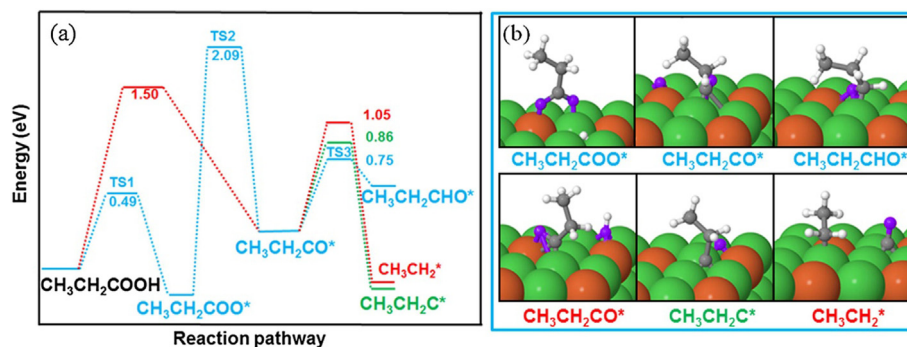


Fig. 7. Reaction mechanism on  $\text{Ni}_3\text{Fe}(111)$  surface (a) and (b) the corresponding transition state (Green, orange, purple, gray and white balls represent Ni, Fe, O, C and H atoms, respectively.) Reprinted with permission from ref [172]. Copyright (2020) Elsevier.



Table 8  
Characteristics of active metal, support and metal support interactions and their influences on natural oils deoxygenation.

Catalyst site	Characteristics	Influences
Active metal	With high C-C bond cleavage activity (e.g., Pt, Ni)	Favoring C <sub>n-1</sub> alkanes formation, not suitable for fatty alcohols production directly
	With relatively high HDO activity (e.g., Pd, Ru, Re, Co)	Favoring C <sub>n</sub> alkanes formation, suitable for fatty alcohols production, temperature-tuned selectivity to both alkanes and fatty alcohols
	With relatively low activity in deoxygenation (e.g., Fe, Mo, Cu, V)	Used as a promoter for synthesizing alkanes or fatty alcohols, enhancing product selectivity via suppressing side-reactions
Support	With high acidity (e.g., HZSM-5, SAPO-11, Y zeolites)	High activity in hydrocracking and isomerization, suitable for producing bio-jet fuels
	With abundant oxygen vacancies (e.g., ZrO <sub>2</sub> , CeO <sub>2</sub> , TiO <sub>2</sub> , MoO <sub>x</sub> )	Promoting substrate adsorption/activation, enhancing the activity of active metals via electron transfer
	With a high specific surface area	Promoting metal dispersion
Metal-support interaction	Strong interactions between active metals and support, forming an abundant metal-support interface	Promoting metal dispersion, promoting electron transfer via M-S interface/bonds, changing the charge/oxidation state of metal sites, creating multifunctional catalytic sites, promoting the adsorption and activation of substrate molecules

reaction temperature should be controlled at a low level to suppress the formation of alkanes. The fatty alcohol intermediate will gradually be converted to alkanes via the DCO or HDO route by increasing the temperature. In some cases, the selectivity of the

target fatty alcohol is high, but the yield is low, which could be improved by adequately prolonging the reaction time. In recent studies, different strategies have been explored for selectively producing fatty alcohols and alkanes with tunable selectivity. Zhou et al. developed a Co/ZrO<sub>2</sub> catalyst for ethyl palmitate deoxygenation to alkanes or alcohols, where the selectivity could be controlled by varying the reaction conditions (reaction temperature and time) [21]. The highest yields to alkanes (82%) and fatty alcohols (86%) could be respectively obtained at 200 °C for 24 h and 240 °C for 8 h. The formation of alkanes and fatty alcohols was proposed to be synergistically catalyzed by Co sites and oxygen vacancy sites of ZrO<sub>2</sub>. In addition, the variation of reaction conditions could also influence the proportion of jet-ranged and diesel-ranged hydrocarbons. Li et al. reported a NiO-Li-ZSM-5 catalyst for waste oil hydrogenation to jet fuels [49]. They found that the reaction temperature, time and hydrogen pressure could influence the distribution of the reaction products. They also concluded that the jet fuel fraction rose gradually with an increase in the reaction temperature, time or hydrogen pressure.

The nature of the active metals could affect the selectivity of target products from natural oils deoxygenation. Active metals with high activity in DCO and HDO, such as Pt and Ni, might not be very suitable for producing fatty alcohols because the formed alcohol intermediates will be quickly converted to alkanes [68,82,110]. However, their activity could also be modified with appropriate supporting materials and promoters (Table 8). To design catalysts with tunable selectivity to alkanes or alcohols, selecting active metals with mild activities might be important. In addition, active metals such as Pd, Ru, Re, Cu and Co are applicable for synthesizing alcohols due to their mild bond cleavage activity [70,134,166,167]. Based on recent studies, alkanes can hardly be formed on monometallic Cu-based catalysts, whereas Ru, Pd, Co and Re are suitable for synthesizing alkanes and fatty alcohols by simply changing the reaction conditions [70,176].

Possible sites on catalysts responsible for the essential steps in natural oils deoxygenation are illustrated in Fig. 9. Taking a fatty ester as a model of substrates, the hydrogenolysis/

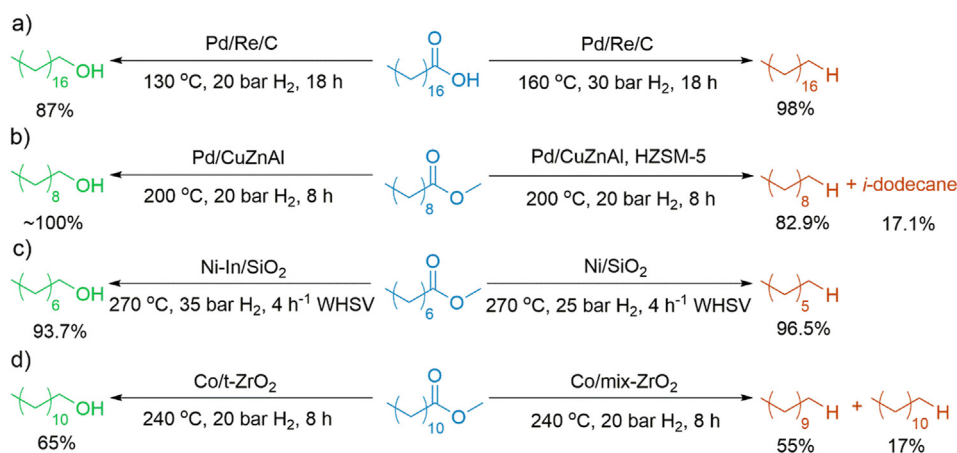


Fig. 8. Typical examples of fatty acid/ester deoxygenation with tunable selectivity adapted from (a) ref. [164], (b) ref. [165], (c) ref. [72], and (d) ref. [134] (the percentages in the graph are the yields of product).



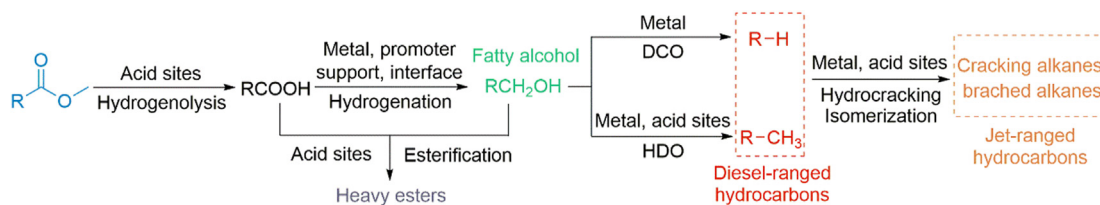


Fig. 9. Possible sites on catalysts responsible for important steps in natural oil deoxygenation.

hydrolysis of a fatty ester to a fatty acid is catalyzed by the acid sites of the catalyst [20,28,134]. It has been reported in recent studies that the metal sites cooperating with the promoter/support/metal-support interface are responsible for the hydrogenation reaction to produce fatty alcohols [21,70,72]. This is due to the fact that introducing the promoter leads to an electron transfer from the metal site to the support via metal-support interactions, and the adsorption and activation of fatty acid molecules commonly occur in the metal-promoter center or metal-support interface, especially in the metal/oxide interface. The metal electron transfer and metal-support interaction could influence the hydrogen cleavage mode and fatty acids/esters/aldehydes (reaction intermediate) adsorption type, switching the reaction pathway and product selectivity. On the one hand, it has been reported that there are two possibilities for the activation and adsorption of  $H_2$  molecules on the supported-metal catalyst surface: homolytic or heterolytic cleavage to H atoms, where the dual form of both pathways leads to higher activity and fatty alcohols selectivity [167]. On the other hand, three types of configurations exist when the fatty acids/esters/aldehydes are adsorbed on the catalyst surface, i.e., carboxylate,  $\eta^1(C)$ -acyl and  $\eta^2(C, O)$ -aldehyde. The carboxylate and  $\eta^1(C)$ -acyl species are easier decarboxylated and decarbonylated to  $C_{n-1}$  alkanes, whereas the  $\eta^2(C, O)$ -aldehyde intermediate tends to form fatty alcohols via hydrogenation [182–184]. These pathways can be affected by the electron density of the metal and/or support site, thus affecting the product distribution. The undesired intermediate product, a heavy ester, is usually unavoidably generated from the esterification of the formed fatty acid and alcohol in the presence of acid/base sites of the catalyst [134]. For obtaining diesel-ranged alkanes, the subsequent decarbonylation requires the participation of a metal site, whereas the hydrodeoxygenation is catalyzed by both acid and metal sites for the development of dehydration-hydrogenation reactions [20,134]. In addition, the hydrocracking and isomerization of linear alkanes require metal sites combined with strong acid sites to obtain lighter and branched alkanes, which are the main components of jet fuels [47,49]. The supporting materials are important for exerting the acidity and basicity of the catalysts and generating metal-support interfaces. To control the selectivity toward different target products, varying the types of supporting materials might be viable. Recently, several studies have reported that it is feasible to control the product selectivity by changing crystal types or synthesis strategies of the reducible oxides supported metal catalysts. These strategies rely on the fact that the metal/oxide interfaces

and the oxygen defects on the oxide surface mainly act as the active center for activating substrate molecules. Zhou and coworkers studied the influence of different  $ZrO_2$  crystalline types on the hydrogenation of methyl laurate over a Co/ $ZrO_2$  catalyst [134]. Co supported on m- $ZrO_2$  with a low BET surface area combined with a low amount of active sites provided the lowest hydrogenation efficiency. In contrast, a Co/t- $ZrO_2$  with a high surface acidity and basicity but a low oxygen vacancy ( $O_v$ ) content exhibited moderate activity. A Co/mix- $ZrO_2$  with strong metal-support interactions, and a high  $O_v$  content showed the most increased activity among the prepared catalysts. Under the same reaction conditions (240 °C, 8 h, 2 MPa  $H_2$ ), Co/t- $ZrO_2$  and Co/m- $ZrO_2$  favored the formation of fatty alcohols, while Co/mix- $ZrO_2$  yielded alkanes as the main products (Fig. 8d). Based on catalyst characterization and kinetic studies, the main reason for the different catalytic activity was the exposed lattice planes of Co and the amount of surface  $O_v$ . Ni et al. studied the effect of support defects on the Ni electron density in Ni/ $ZrO_2$  catalysts for fatty acids hydrogenation [131]. The catalytic tests showed that a m- $ZrO_2$  supported Ni catalyst exhibited high selectivity to fatty alcohols, whereas a Ni/t- $ZrO_2$  catalyst had high selectivity to alkanes. By characterizing the catalysts and conducting DFT calculations, the difference in the selectivity was correlated to the defects in  $ZrO_2$ , which influenced the electron density of metal Ni. Ni with higher electron density favored the hydrogenation of aldehyde intermediates to fatty alcohols, while Ni with lower electron density boosted the DCO of aldehydes to alkanes.

## 6. Conclusions, challenges and opportunities

The chemical transformation of natural oils or related model compounds is one of the most promising routes to obtain sustainable energy and valuable products. This review has collected vital information, covering all work reported to date to provide the readership with an in-depth understanding of a novel and holistic “natural oil refinery”. This new scenario allows gaining the most from renewable resources and opens the door for the selective production of renewable fuels and value-added chemicals independently and/or concurrently to suit the different present and future market needs.

For diesel fuel production, metal-non-metal, noble metal and non-noble metal catalysts have been commonly used. Among these, noble metals (Pt, Pd, Ru) exhibit high catalytic performance to achieve a high yield of hydrocarbons under mild conditions (140–300 °C). In contrast, non-noble metals

and metal-non-metal catalysts are more promising in cost but also show considerable activity (240–400 °C). For bio-jet fuels production, higher reaction temperatures (240–450 °C) and multifunctional catalysts with higher acidity are required. These comprise metal supported on ZSM-5, Y-zeolites, and SAPO-11. In terms of fatty alcohols synthesis, active metals with high C-C cleavage activity (e.g., Pt and Rh) might not be suitable. This incompatibility accounts for fatty alcohol intermediates being rapidly converted to alkanes during the hydrogenation process. In addition, the reaction temperature for synthesizing fatty alcohols is generally lower than that for hydrocarbons production (130–270 °C), and the catalyst acidity should be relatively low to avoid the formation of heavy esters. To control the selectivity to different target products from natural oil hydrogenation, active metals with mild activity and moderate deoxygenation rate are suitable. The selectivity could be controlled by tuning the reaction conditions and adjusting the properties of the supporting materials.

The selective deoxygenation of natural oils and related model compounds to hydrocarbon fuels and value-added fatty alcohols offer challenging research opportunities in the following areas:

- (1) *Developing catalysts with high stability and selectivity to target products.* The deoxygenation process of fatty acids/esters usually yields mixtures of alkanes (from the DCO, HDO and hydrocracking routes) together with fatty alcohols mixed with other by-products. As a result, the purification and separation of the products in the mixtures are required to obtain high purity chemicals, making the process more complex. Therefore, more efficient catalysts need to be developed to obtain products with high purity directly. In addition, catalyst stability is one of the most significant challenges in heterogeneous catalysis. Catalysts with high stability and excellent recyclability under reaction conditions are promising for reducing the material cost. Gaining more insights into the morphological and chemical changes occurring in the catalyst during natural oil deoxygenation is necessary. It is vital to understand how and to what extent the alterations occurring in the catalysts during the process influence their activity and selectivity. This could be beneficial for designing stable catalysts for natural oils deoxygenation.
- (2) *Studying the reaction mechanisms by in-situ/operando characterizations technologies.* In recent studies, most reaction mechanisms over specific catalysts in natural oil deoxygenation are proposed based on some ex-situ characterization techniques and DFT calculations. To gain more insights and provide fundamental details into molecular structure-activity/selectivity relationships, in-situ/operando characterization technologies are applicable to monitor the atomic dynamics, surface molecular adsorption, surface elemental composition and valence state during the reaction. These can include in-situ/operando scanning/transmission electron microscopy, frontier-transform infrared spectroscopy and AP-XPS [185].
- (3) *Making the process greener.* Recent studies on natural oils deoxygenation to hydrocarbon fuels and fatty alcohols were conducted in organic solvent systems (e.g., *n*-heptane, cyclohexane, *n*-dodecane). These solvents are harmful to human beings and the environment if mismanaged. Therefore, developing other technologies using greener solvents or solvent-free systems is required. Among these, water is considered one of the greenest and readily available solvents. To conduct the deoxygenation process under hydrothermal conditions, the hydrothermal stability of catalysts should be taken into consideration because some materials are easily deactivated under hydrothermal conditions. The most common deactivation mechanisms include support hydrolysis or collapse, leaching, sintering and poisoning. Although some recent studies have developed a solvent-free process for natural oils deoxygenation in fix-bed or continuous-bed reactors, the reactions are usually conducted at high temperatures (over 300 °C). Thus, energy-efficient solvent-free processes are also required to be developed. In addition, catalysts containing metal sulfides and harmful metals (e.g., Cr) should be avoided.

### Conflict of interest

The authors declare that they have no known competing financial interests or personal relationships that could have appeared to influence the work reported in this paper.

### Acknowledgments

This work was financially supported by the National Natural Science Foundation of China (No. 21536007) and the 111 Project (B17030). Yingdong Zhou acknowledges the support from China Scholarship Council (CSC No. 202006240156). Javier Remón is grateful to the Spanish Ministry of Science, Innovation and Universities for the Juan de la Cierva (JdC) fellowships (Grant Numbers FJCI-2016-30847 and IJC2018-037110-I) awarded.

### References

- [1] B. Liu, D. Rajagopal, *Nat. Energy* 4 (2019) 700–708.
- [2] J. Dai, *Green Energy Environ* 6 (2021) 22–32.
- [3] S. Kim, J. Lauterbach, E. Sasmaz, *ACS Catal.* 11 (2021) 8247–8260.
- [4] Y. Xu, V. Ramanathan, D.G. Victor, *Nature* 564 (2018) 30–32.
- [5] Danish, Z. Wang, *Sci. Total Environ.* 670 (2019) 1075–1083.
- [6] Q. Yang, H. Zhou, P. Bartocci, F. Fantozzi, O. Masek, F.A. Agblevor, Z. Wei, H. Yang, H. Chen, X. Lu, G. Chen, C. Zheng, C.P. Nielsen, M.B. Mcelroy, *Nat. Commun.* 12 (2021) 1698.
- [7] S. Zhang, S.-F. Jiang, B.-C. Huang, X.-C. Shen, W.-J. Chen, T.-P. Zhou, H.-Y. Cheng, B.-H. Cheng, C.-Z. Wu, W.-W. Li, H. Jiang, H.-Q. Yu, *Nat. Sustain.* 3 (2020) 753–760.
- [8] P. Sudarsanam, R. Zhong, S. Van Den Bosch, S.M. Coman, V.I. Parvulescu, B.F. Sels, *Chem. Soc. Rev.* 47 (2018) 8349–8402.
- [9] M. Antar, D. Lyu, M. Nazari, A. Shah, X. Zhou, D.L. Smith, *Renew. Sustain. Energy Rev.* 139 (2021) 110691.
- [10] J.H. Clark, *Green Chem.* 21 (2019) 1168–1170.
- [11] J. Remón, F. Santomauro, C.J. Chuck, A.S. Matharu, J.H. Clark, *Green Chem.* 20 (2018) 4507–4520.

- [12] A. Lorente, J. Remón, V.L. Budarin, P. Sánchez-Verdú, A. Moreno, J.H. Clark, *Energy Convers. Manag.* 185 (2019) 410–430.
- [13] S.C. De Vries, G.W.J. Van De Ven, M.K. Van Ittersum, K.E. Giller, *Biomass Bioenergy* 34 (2010) 588–601.
- [14] S.K. Bhatia, S.-H. Kim, J.-J. Yoon, Y.-H. Yang, *Energy Convers. Manag.* 148 (2017) 1142–1156.
- [15] I. Davila, J. Remon, P. Gullon, J. Labidi, V. Budarin, *Bioresour. Technol.* 289 (2019) 121726.
- [16] J. Remón, A.S. Matharu, J.H. Clark, *Energy Convers. Manag.* 165 (2018) 634–648.
- [17] J. Dai, F. Li, X. Fu, *ChemSusChem* 13 (2020) 6498–6508.
- [18] K.W. Chew, J.Y. Yap, P.L. Show, N.H. Suan, J.C. Juan, T.C. Ling, D.-J. Lee, J.-S. Chang, *Bioresour. Technol.* 229 (2017) 53–62.
- [19] Y. Zhou, L. Liu, M. Li, C. Hu, *Bioresour. Technol.* 344 (2022) 126371.
- [20] J. Chen, H. Shi, L. Li, K. Li, *Appl. Catal. B Environ.* 144 (2014) 870–884.
- [21] Y. Zhou, X. Liu, P. Yu, C. Hu, *Fuel* 278 (2020) 118295.
- [22] L.M.L. Laurens, J. Markham, D.W. Templeton, E.D. Christensen, S. Van Wychem, E.W. Vadelius, M. Chen-Glasser, T. Dong, R. Davis, P.T. Pienkos, *Energy Environ. Sci.* 10 (2017) 1716–1738.
- [23] P. Appaiah, L. Sunil, P.K. Prasanth Kumar, A.G. Gopala Krishna, *J. Am. Oil Chem. Soc.* 91 (2014) 917–924.
- [24] J. Remón, P. Arcelus-Arriaga, L. García, J. Arauzo, *Appl. Energy* 228 (2018) 2275–2287.
- [25] X.Y. Ooi, W. Gao, H.C. Ong, H.V. Lee, J.C. Juan, W.H. Chen, K.T. Lee, *Renew. Sustain. Energy Rev.* 112 (2019) 834–852.
- [26] R.K. Saini, Y.S. Keum, *Life Sci.* 203 (2018) 255–267.
- [27] Z. Luo, Q. Bing, J. Kong, J.-Y. Liu, C. Zhao, *Catal. Sci. Technol.* 8 (2018) 1322–1332.
- [28] M. Peroni, I. Lee, X. Huang, E. Baráth, O.Y. Gutiérrez, J.A. Lercher, *ACS Catal.* 7 (2017) 6331–6341.
- [29] H. Jeong, H.B. Bathula, T.W. Kim, G.B. Han, J.H. Jang, B. Jeong, Y.-W. Suh, *ACS Sustain. Chem. Eng.* 9 (2021) 1193–1202.
- [30] N. Asikin-Mijan, J.M. Ooi, G. Abdulkareem-Alsultan, H.V. Lee, M.S. Mastuli, N. Mansir, F.A. Alharthi, A.A. Alghamdi, Y.H. Taufiq-Yap, *J. Clean. Prod.* 249 (2020) 119381.
- [31] N. Numwong, P. Prabnasak, P. Prayoonpunrat, P. Triphatthanaphong, C. Thunyaratchatanon, T. Mochizuki, S.-Y. Chen, A. Luengnaruemitchai, T. Sooknoi, *Fuel Process. Technol.* 203 (2020) 106393.
- [32] P. Albrand, C. Julcour, F. Veyrine, A.-M. Billet, *Chem. Eng. J.* 420 (2021) 129854.
- [33] V. Váchová, D. Toullis, P. Straka, P. Šimáček, M. Staš, A. Gdovin, Z. Beňo, J. Blažek, *Energy Fuels* 34 (2020) 9609–9619.
- [34] G. Xu, Y. Zhang, Y. Fu, Q. Guo, *ACS Catal.* 7 (2017) 1158–1169.
- [35] M. Toda, A. Takagaki, M. Okamura, J.N. Kondo, S. Hayashi, K. Domen, M. Hara, *Nature* 438 (2005) 178, 178.
- [36] X. Zhang, W. Xiong, Z. Yin, Y. Chen, Y. Wu, X. Hu, *Green Energy Environ* 7 (2022) 137–144.
- [37] J.M. Marchetti, V.U. Miguel, A.F. Errazu, *Renew. Sustain. Energy Rev.* 11 (2007) 1300–1311.
- [38] J. Remón, J. Ruiz, M. Oliva, L. García, J. Arauzo, *Chem. Eng. J.* 299 (2016) 431–448.
- [39] A. Gaurav, S. Dumas, C.T.Q. Mai, F.T.T. Ng, *Green Energy Environ* 4 (2019) 328–341.
- [40] A. Demirbas, *Energy Pol.* 35 (2007) 4661–4670.
- [41] X. Yao, T.J. Strathmann, Y. Li, L.E. Cronmiller, H. Ma, J. Zhang, *Green Chem.* 23 (2021) 1114–1129.
- [42] C. Gutiérrez-Antonio, F.I. Gómez-Castro, J.A. De Lira-Flores, S. Hernández, *Renew. Sustain. Energy Rev.* 79 (2017) 709–729.
- [43] Y. Chen, Y. Zhou, R. Zhang, C. Hu, *Mol. Catal.* 484 (2020) 110729.
- [44] Y. Zhou, M. Li, Y. Chen, C. Hu, *J. Appl. Phycol.* 33 (2021) 101–110.
- [45] M.A. Sánchez, G.C. Torres, V.A. Mazzieri, C.L. Pieck, *J. Chem. Technol. Biotechnol.* 92 (2017) 27–42.
- [46] M. Tamura, Y. Nakagawa, K. Tomishige, *Asian J. Org. Chem.* 9 (2020) 1–19.
- [47] M. Alherbawi, G. Mckay, H.R. Mackey, T. Al-Ansari, *Renew. Sustain. Energy Rev.* 135 (2021) 110396.
- [48] F. Long, W. Liu, X. Jiang, Q. Zhai, X. Cao, J. Jiang, J. Xu, *Renew. Sustain. Energy Rev.* 148 (2021) 111269.
- [49] M. Li, J. Fu, S. Xing, L. Yang, X. Zhang, P. Lv, Z. Wang, Z. Yuan, *Appl. Catal. B Environ.* 260 (2020) 118114.
- [50] E. Baldauf, A. Sievers, T. Willner, *Biofuels* 8 (2016) 555–564.
- [51] B.P. Pattanaik, R.D. Misra, *Renew. Sustain. Energy Rev.* 73 (2017) 545–557.
- [52] G.J.S. Dawes, E.L. Scott, J. Le Nôtre, J.P.M. Sanders, J.H. Bitter, *Green Chem.* 17 (2015) 3231–3250.
- [53] M. Ameen, M.T. Azizan, S. Yusup, A. Ramli, M. Yasir, *Renew. Sustain. Energy Rev.* 80 (2017) 1072–1088.
- [54] M.C. Vásquez, E.E. Silva, E.F. Castillo, *Biomass Bioenergy* 105 (2017) 197–206.
- [55] S. Janampelli, S. Darbha, *Catal. Surv. Asia* 23 (2019) 90–101.
- [56] X. Zhao, L. Wei, S. Cheng, J. Julson, *Catalysts* 7 (2017) 83.
- [57] N. Hongloi, P. Prapainainar, C. Prapainainar, *Mol. Catal.* (2021) 111696, <https://doi.org/10.1016/j.mcat.2021.111696>.
- [58] R.W. Gosselink, S.A. Hollak, S.W. Chang, J. Van Haveren, K.P. De Jong, J.H. Bitter, D.S. Van Es, *ChemSusChem* 6 (2013) 1576–1594.
- [59] Z. Lu, V. Cherepakhin, T. Kapenstein, T.J. Williams, *ACS Sustain. Chem. Eng.* 6 (2018) 5749–5753.
- [60] J.A. Melero, M.M. Clavero, G. Calleja, A. García, R.N. Miravalles, T. Galindo, *Energy Fuels* 24 (2010) 707–717.
- [61] L. Liu, Y. Zhou, L. Guo, G. Li, C. Hu, *ChemSusChem* 14 (2021) 3935–3944.
- [62] D. Bolonio, M.-J. García-Martínez, M.F. Ortega, M. Lapuerta, J. Rodríguez-Fernández, L. Canoira, *Renew. Energy* 132 (2019) 278–283.
- [63] M.F. Kamaruzaman, Y.H. Taufiq-Yap, D. Derawi, *Biomass Bioenergy* 134 (2020) 105476.
- [64] R. Loe, Y. Lavoignat, M. Maier, M. Abdallah, T. Morgan, D. Qian, R. Pace, E. Santillan-Jimenez, M. Crocker, *Catalysts* 9 (2019) 123.
- [65] T.T. Nguyen, M.K. Lam, Y. Uemura, N. Mansor, J.W. Lim, P.L. Show, I.S. Tan, S. Lim, *Fuel* 272 (2020) 117718.
- [66] H. Zhong, C. Jiang, X. Zhong, J. Wang, B. Jin, G. Yao, L. Luo, F. Jin, *J. Clean. Prod.* 209 (2019) 1228–1234.
- [67] S. Thongkumkoon, W. Kiatkittipong, U.W. Hartley, N. Laosiripojana, P. Daorattanachai, *Renew. Energy* 140 (2019) 111–123.
- [68] B. Peng, X. Yuan, C. Zhao, J.A. Lercher, *J. Am. Chem. Soc.* 134 (2012) 9400–9405.
- [69] J. Hancsók, T. Kasza, S. Kovács, P. Solymosi, A. Holló, *J. Clean. Prod.* 34 (2012) 76–81.
- [70] Z. Zhang, M. Jing, H. Chen, F. Okejiri, J. Liu, Y. Leng, H. Liu, W. Song, Z. Hou, X. Lu, J. Fu, J. Liu, *ACS Catal.* 10 (2020) 9098–9108.
- [71] R. Nie, Y. Tao, Y. Nie, T. Lu, J. Wang, Y. Zhang, X. Lu, C.C. Xu, *ACS Catal.* 11 (2021) 1071–1095.
- [72] L. Wang, X. Niu, J. Chen, *Appl. Catal. B Environ.* 278 (2020) 119293.
- [73] N. Krobkrong, V. Itthibenchapong, P. Khongpracha, K. Faungnawakij, *Energy Convers. Manag.* 167 (2018) 1–8.
- [74] C.A. Fonseca Benítez, V.A. Mazzieri, C.R. Vera, V.M. Benitez, C.L. Pieck, *React. Chem. Eng.* 6 (2021) 726–746.
- [75] W. Fang, A. Riisager, *Green Chem.* 23 (2021) 670–688.
- [76] I. Coronado, M. Stekrova, L. García Moreno, M. Reinikainen, P. Simell, R. Karinen, J. Lehtonen, *Biomass Bioenergy* 106 (2017) 29–37.
- [77] M. Shahinuzzaman, Z. Yaakob, Y. Ahmed, *Renew. Sustain. Energy Rev.* 77 (2017) 1375–1384.
- [78] S. Khan, A.N. Kay Lup, K.M. Qureshi, F. Abnisa, W.M.A. Wan Daud, M.F.A. Patah, *J. Anal. Appl. Pyrolysis* 140 (2019) 1–24.
- [79] E.N. Vlasova, A.A. Porsin, P.V. Aleksandrov, A.L. Nuzhdin, G.A. Bukhtiyarova, *Catal. Today* 378 (2020) 119–125.
- [80] M. Peroni, G. Mancino, E. Baráth, O.Y. Gutiérrez, J.A. Lercher, *Appl. Catal. B Environ.* 180 (2016) 301–311.
- [81] C.-C. Tran, D. Akmach, S. Kaliaguine, *Green Chem.* 22 (2020) 6424–6436.
- [82] D.-P. Phan, V.N. Le, T.H. Nguyen, H.B. Kim, E.D. Park, J. Kim, E.Y. Lee, *J. Catal.* 400 (2021) 283–293.
- [83] T. Hengsawad, T. Jindarat, D.E. Resasco, S. Jongpatiwut, *Appl. Catal. Gen.* 566 (2018) 74–86.



- [84] J. Zhang, X. Huo, Y. Li, T.J. Strathmann, ACS Sustain. Chem. Eng. 7 (2019) 14400–14410.
- [85] F. Deng, J. Huang, E.E. Ember, K. Achterhold, M. Dierolf, A. Jentys, Y. Liu, F. Pfeiffer, J.A. Lercher, ACS Catal. 11 (2021) 14625–14634.
- [86] K. Jenišťová, I. Hachemi, P. Mäki-Arvela, N. Kumar, M. Peurla, L. Čapek, J. Wärnä, D.Y. Murzin, Chem. Eng. J. 316 (2017) 401–409.
- [87] M. Safa Gamal, N. Asikin-Mijan, M. Arumugam, U. Rashid, Y.H. Taufiq-Yap, J. Anal. Appl. Pyrolysis 144 (2019) 104690.
- [88] J. Zhong, Q. Deng, T. Cai, X. Li, R. Gao, J. Wang, Z. Zeng, G. Dai, S. Deng, Fuel 292 (2021) 120248.
- [89] J. Liang, T. Chen, J. Liu, Q. Zhang, W. Peng, Y. Li, F. Zhang, X. Fan, Chem. Eng. J. 391 (2020) 123472.
- [90] S.T. Oyama, T. Gott, H. Zhao, Y.-K. Lee, Catal. Today 143 (2009) 94–107.
- [91] A.M. Robinson, J.E. Hensley, J.W. Medlin, ACS Catal. 6 (2016) 5026–5043.
- [92] S. Ding, C.M.A. Parlett, X. Fan, Mol. Catal. (2021) 111492, <https://doi.org/10.1016/j.mcat.2021.111492>.
- [93] M.F. Wagenhofer, E. Baráth, O.Y. Gutiérrez, J.A. Lercher, ACS Catal. 7 (2017) 1068–1076.
- [94] X. Du, W. Liang, X. Hao, K. Zhou, H. Yang, X. Lei, D. Li, C. Hu, Catal. Today 367 (2021) 83–94.
- [95] Y. Shi, M. Li, Y. Yu, B. Zhang, Energy Environ. Sci. 13 (2020) 4564–4582.
- [96] Y. Liu, L. Yao, H. Xin, G. Wang, D. Li, C. Hu, Appl. Catal. B Environ. 174–175 (2015) 504–514.
- [97] H. Xin, K. Guo, D. Li, H. Yang, C. Hu, Appl. Catal. B Environ. 187 (2016) 375–385.
- [98] Y. Ma, G. Guan, X. Hao, J. Cao, A. Abudula, Renew. Sustain. Energy Rev. 75 (2017) 1101–1129.
- [99] J. Pang, J. Sun, M. Zheng, H. Li, Y. Wang, T. Zhang, Appl. Catal. B Environ. 254 (2019) 510–522.
- [100] X. Du, K. Zhou, L. Zhou, X. Lei, H. Yang, D. Li, C. Hu, J. Energy Chem. 61 (2021) 425–435.
- [101] S.a.W. Hollak, R.W. Gosselink, D.S. Van Es, J.H. Bitter, ACS Catal. 3 (2013) 2837–2844.
- [102] Z. Wei, J. Wang, S. Mao, D. Su, H. Jin, Y. Wang, F. Xu, H. Li, Y. Wang, ACS Catal. 5 (2015) 4783–4789.
- [103] F. Wang, J. Jiang, K. Wang, Q. Zhai, F. Long, P. Liu, J. Feng, H. Xia, J. Ye, J. Li, J. Xu, Appl. Catal. B Environ. 242 (2019) 150–160.
- [104] T. Burimsithigul, B. Yoosuk, C. Ngamcharussrivichai, P. Prasassarakich, Renew. Energy 163 (2021) 1648–1659.
- [105] M. Ruangdomsakul, N. Osakoo, C. Keawkumay, C. Kongmanklang, T. Wutburee, S. Kiatphuengporn, K. Faungnawakij, N. Chanlek, J. Wittayakun, P. Khemthong, Catal. Today 367 (2021) 153–164.
- [106] S. Phimsen, W. Kiatkittipong, H. Yamada, T. Tagawa, K. Kiatkittipong, N. Laosiripojana, S. Assabumrungrat, Energy Convers. Manag. 151 (2017) 324–333.
- [107] X. Chen, X. Chen, C. Li, C. Liang, Sustain. Energy Fuels 4 (2020) 2370–2379.
- [108] K.W. Cheah, S. Yusup, A.C.M. Loy, B.S. How, V. Skoulou, M.J. Taylor, Mol. Catal. (2021) 111469, <https://doi.org/10.1016/j.mcat.2021.111469>.
- [109] R. Van Lent, S.V. Auras, K. Cao, A.J. Walsh, M.A. Gleeson, L.B.F. Juurlink, Science 363 (2019) 155–157.
- [110] S. Lei, S. Qin, B. Li, C. Zhao, J. Catal. 400 (2021) 244–254.
- [111] C. Sarkar, S.C. Shit, D.Q. Dao, J. Lee, N.H. Tran, R. Singuru, K. An, D.N. Nguyen, Q.V. Le, P.N. Amaniampong, A. Drif, F. Jerome, P.T. Huyen, T.T.N. Phan, D.-V.N. Vo, N. Thanh Binh, Q.T. Trinh, M.P. Sherburne, J. Mondal, Green Chem. 22 (2020) 2049–2068.
- [112] H. Liu, J. Han, Q. Huang, H. Shen, L. Lei, Z. Huang, Z. Zhang, Z.K. Zhao, F. Wang, Ind. Eng. Chem. Res. 59 (2020) 17440–17450.
- [113] A. Ali, C. Zhao, Chin. J. Catal. 41 (2020) 1174–1185.
- [114] L. Zhou, W. Lin, K. Liu, Z. Wang, Q. Liu, H. Cheng, C. Zhang, M. Arai, F. Zhao, Catal. Sci. Technol. 10 (2020) 222–230.
- [115] L. Yang, M.A. Carreon, ACS Appl. Mater. Interfaces 9 (2017) 31993–32000.
- [116] Y. Liu, X. Yang, H. Liu, Y. Ye, Z. Wei, Appl. Catal. B Environ. 218 (2017) 679–689.
- [117] Z. Huang, Z. Zhao, C. Zhang, J. Lu, H. Liu, N. Luo, J. Zhang, F. Wang, Nat. Catal. 3 (2020) 170–178.
- [118] L. Zhao, B. Li, C. Zhao, ACS Sustain. Chem. Eng. 9 (2021) 12970–12977.
- [119] S. Xie, C. Jia, A. Prakash, M.I. Palafox, J. Pfaendtner, H. Lin, ACS Catal. 9 (2019) 3753–3763.
- [120] X. Cao, J. Zhao, F. Long, X. Zhang, J. Xu, J. Jiang, Appl. Catal. B Environ. 305 (2022) 121068.
- [121] J.-H. Guo, G.-Y. Xu, F. Shen, Y. Fu, Y. Zhang, Q.-X. Guo, Green Chem. 17 (2015) 2888–2895.
- [122] H. Baek, K. Kashimura, T. Fujii, S. Tsubaki, Y. Wada, S. Fujikawa, T. Sato, Y. Uozumi, Y.M.A. Yamada, ACS Catal. 10 (2020) 2148–2156.
- [123] S. Lycourghiotis, E. Kordouli, L. Sygellou, K. Bourikas, C. Kordulis, Appl. Catal. B Environ. 259 (2019) 118059.
- [124] J.-O. Shim, K.-W. Jeon, W.-J. Jang, H.-S. Na, J.-W. Cho, H.-M. Kim, Y.-L. Lee, D.-W. Jeong, H.-S. Roh, C.H. Ko, Appl. Catal. B Environ. 239 (2018) 644–653.
- [125] C. Papadopoulos, E. Kordouli, L. Sygellou, K. Bourikas, C. Kordulis, A. Lycourghiotis, Fuel Process. Technol. 217 (2021) 106820.
- [126] D. Jiraroj, O. Jirarattanapochai, W. Anutrasakda, J.S.M. Samec, D.N. Tungasmita, Appl. Catal. B Environ. 291 (2021) 120050.
- [127] V.K. Soni, S. Dhara, R. Krishnapriya, G. Choudhary, P.R. Sharma, R.K. Sharma, Fuel 266 (2020) 117065.
- [128] V.K. Soni, P.R. Sharma, G. Choudhary, S. Pandey, R.K. Sharma, ACS Sustain. Chem. Eng. 5 (2017) 5351–5359.
- [129] D. Zeng, Y. Li, H. Ma, F. Cui, J. Zhang, ACS Sustain. Chem. Eng. 9 (2021) 15612–15622.
- [130] J. Wang, L. Xu, R. Nie, X. Lyu, X. Lu, Fuel 265 (2020) 116913.
- [131] J. Ni, W. Leng, J. Mao, J. Wang, J. Lin, D. Jiang, X. Li, Appl. Catal. B Environ. 253 (2019) 170–178.
- [132] S. Xing, Y. Liu, X. Liu, M. Li, J. Fu, P. Liu, P. Lv, Z. Wang, Appl. Catal. B Environ. 269 (2020) 118718.
- [133] H. Yan, S. Yao, T. Zhang, D. Li, X. Tang, M. Chen, Y. Zhou, M. Zhang, Y. Liu, X. Zhou, X. Feng, X. Chen, C. Yang, Appl. Catal. B Environ. 306 (2022) 121138.
- [134] Y. Zhou, L. Liu, G. Li, C. Hu, ACS Catal. 11 (2021) 7099–7113.
- [135] E. Kordouli, B. Pawelec, K. Bourikas, C. Kordulis, J.L.G. Fierro, A. Lycourghiotis, Appl. Catal. B Environ. 229 (2018) 139–154.
- [136] Z. Zhang, H. Chen, C. Wang, K. Chen, X. Lu, P. Ouyang, J. Fu, Fuel 230 (2018) 211–217.
- [137] Z. Zhang, Q. Yang, H. Chen, K. Chen, X. Lu, P. Ouyang, J. Fu, J.G. Chen, Green Chem. 20 (2018) 197–205.
- [138] H. Xin, H. Yang, X. Lei, X. Du, K. Zhou, D. Li, C. Hu, Ind. Eng. Chem. Res. 59 (2020) 17373–17386.
- [139] C.P. Ferraz, A. Kiméné, K. Silva Vargas, S. Heyte, C. Durlin, O. Simon, F. Dumeignil, S. Paul, R. Wojcieszak, Catal. Sci. Technol. 11 (2021) 3025–3038.
- [140] Y. Nakagawa, M. Tamura, K. Tomishige, Fuel Process. Technol. 193 (2019) 404–422.
- [141] M.Y. Kim, J.-K. Kim, M.-E. Lee, S. Lee, M. Choi, ACS Catal. 7 (2017) 6256–6267.
- [142] J. Cheng, Z. Zhang, X. Zhang, Z. Fan, J. Liu, J. Zhou, Int. J. Hydrogen Energy 44 (2019) 11765–11773.
- [143] X. Du, D. Li, H. Xin, W. Zhou, R. Yang, K. Zhou, C. Hu, Energy Technol. 7 (2019) 1800809.
- [144] H. Yang, X. Du, X. Lei, K. Zhou, Y. Tian, D. Li, C. Hu, Appl. Energy 301 (2021) 117469.
- [145] S. Gong, A. Shinozaki, E.W. Qian, Ind. Eng. Chem. Res. 51 (2012) 13953–13960.
- [146] K. Lee, M.-E. Lee, J.-K. Kim, B. Shin, M. Choi, J. Catal. 379 (2019) 180–190.
- [147] A. Ishihara, K. Takemoto, T. Hashimoto, Fuel 289 (2021) 119885.
- [148] V. Itthibenchapong, A. Srifa, R. Kaewmeesri, P. Kidkhunthod, K. Faungnawakij, Energy Convers. Manag. 134 (2017) 188–196.
- [149] Q. Tan, Y. Cao, J. Li, Renew. Energy 150 (2020) 370–381.
- [150] E.S.K. Why, H.C. Ong, H.V. Lee, W.-H. Chen, N. Asikin-Mijan, M. Varman, Energy Convers. Manag. 243 (2021) 114311.

- [151] P. Chintakanan, T. Vitidsant, P. Reubroycharoen, P. Kuchonthara, T. Kida, N. Hinchiranan, *Fuel* 293 (2021) 120472.
- [152] J. Zhang, Y. Shi, H. Cao, Y. Wu, M. Yang, *Appl. Catal. Gen.* 608 (2020) 117847.
- [153] C.-H. Lin, Y.-K. Chen, W.-C. Wang, *Fuel* 260 (2020) 116345.
- [154] J. Remón, G. Zhu, V.L. Budarin, J.H. Clark, *Green Chem.* 20 (2018) 2624–2636.
- [155] T. Turek, D.L. Trimm, N.W. Cant, *Catal. Rev.* 36 (1994) 645–683.
- [156] V.O. Rodina, D.Y. Ermakov, A.A. Saraev, S.I. Reshetnikov, V.A. Yakovlev, *Appl. Catal. B Environ.* 209 (2017) 611–620.
- [157] M.A. Sánchez, M.A. Vicerich, V.A. Mazzieri, E. Gioria, L.B. Gutierrez, C.L. Pieck, *Can. J. Chem. Eng.* 97 (2019) 2333–2339.
- [158] M.A. Sánchez, Y. Pouilloux, V.A. Mazzieri, C.L. Pieck, *Appl. Catal. Gen.* 467 (2013) 552–558.
- [159] K. De Oliveira Vigier, Y. Pouilloux, J. Barrault, *Catal. Today* 195 (2012) 71–75.
- [160] M.A. Sánchez, V.A. Mazzieri, M.A. Vicerich, C.R. Vera, C.L. Pieck, *Ind. Eng. Chem. Res.* 54 (2015) 6845–6854.
- [161] C.A. Fonseca Benítez, V.A. Mazzieri, M.A. Sánchez, V.M. Benitez, C.L. Pieck, *Appl. Catal. Gen.* 584 (2019) 117149.
- [162] D. Han, W. Yin, D. Luo, H. He, S. Wang, S. Xia, *Fuel* 305 (2021) 121545.
- [163] Y. Pouilloux, F. Autin, A. Piccirilli, C. Guimon, J. Barrault, *Appl. Catal. Gen.* 169 (1998) 65–75.
- [164] J. Ullrich, B. Breit, *ACS Catal.* 8 (2017) 785–789.
- [165] Z. Guo, F. Zhou, H. Wang, X. Liu, G. Xu, Y. Zhang, Y. Fu, *Green Chem.* 21 (2019) 5046–5052.
- [166] Y. Takeda, M. Tamura, Y. Nakagawa, K. Okumura, K. Tomishige, *ACS Catal.* 5 (2015) 7034–7047.
- [167] L.M. Martínez-Prieto, M. Puche, C. Cerezo-Navarrete, B. Chaudret, *J. Catal.* 377 (2019) 429–437.
- [168] A. Ali, B. Li, Y. Lu, C. Zhao, *Green Chem.* 21 (2019) 3059–3064.
- [169] D. Han, W. Yin, S. Wang, S. Xia, *ACS Sustain. Chem. Eng.* 9 (2021) 15027–15041.
- [170] X. Cao, F. Long, Q. Zhai, J. Zhao, J. Xu, J. Jiang, *Fuel* 298 (2021) 120829.
- [171] X. Cao, F. Long, G. Zhang, J. Xu, J. Jiang, *ACS Sustain. Chem. Eng.* 9 (2021) 9789–9801.
- [172] X. Kong, Z. Fang, X. Bao, Z. Wang, S. Mao, Y. Wang, *J. Catal.* 367 (2018) 139–149.
- [173] J. Wang, R. Nie, L. Xu, X. Lyu, X. Lu, *Green Chem.* 21 (2019) 314–320.
- [174] B. Rozmyslowicz, A. Kirilin, A. Aho, H. Manyar, C. Hardacre, J. Wärnå, T. Salmi, D.Y. Murzin, *J. Catal.* 328 (2015) 197–207.
- [175] L. Wu, L. Li, B. Li, C. Zhao, *Chem. Commun.* 53 (2017) 6152–6155.
- [176] Y. Yao, X. Wu, O.Y. Gutiérrez, J. Ji, P. Jin, S. Wang, Y. Xu, Y. Zhao, S. Wang, X. Ma, J.A. Lercher, *Appl. Catal. B Environ.* 267 (2020) 118698.
- [177] S. Song, D. Wang, L. Di, C. Wang, W. Dai, G. Wu, N. Guan, L. Li, *Chin. J. Catal.* 39 (2018) 250–257.
- [178] S. Yao, T. Zhang, X. Tang, D. Li, W. Zhang, D. Lin, R. Li, H. Yan, Y. Liu, X. Feng, X. Chen, X. Zhou, C. Yang, *Energy Fuels* 35 (2021) 9970–9982.
- [179] X. Gou, F. Okejiri, Z. Zhang, M. Liu, J. Liu, H. Chen, K. Chen, X. Lu, P. Ouyang, J. Fu, *Fuel Process. Technol.* 205 (2020) 106426.
- [180] L. Hermida, A.Z. Abdullah, A.R. Mohamed, *Renew. Sustain. Energy Rev.* 42 (2015) 1223–1233.
- [181] P. Kumar, S.R. Yenumala, S.K. Maity, D. Shee, *Appl. Catal. Gen.* 471 (2014) 28–38.
- [182] Z. Pan, R. Wang, J. Chen, *Appl. Catal. B Environ.* 224 (2018) 88–100.
- [183] J. Yang, S. Li, L. Zhang, X. Liu, J. Wang, X. Pan, N. Li, A. Wang, Y. Cong, X. Wang, T. Zhang, *Appl. Catal. B Environ.* 201 (2017) 266–277.
- [184] S. Sithisa, T. Pham, T. Prasomsri, T. Sooknoi, R.G. Mallinson, D.E. Resasco, *J. Catal.* 280 (2011) 17–27.
- [185] X. Li, X. Yang, J. Zhang, Y. Huang, B. Liu, *ACS Catal.* 9 (2019) 2521–2531.